University of Nevada
Reno

The Effects of Pretreatment Conditions, Ionic Strength, Collector Type, Chain Length and Temperature on the Cationic Flotation of Oxide Minerals

A thesis submitted in partial fulfillment of the
requirements for the degree of Master of Science
in Metallurgical Engineering

by
Jeffrey Lynn Scott

May, 1983

The thesis of Jeffrey L. Scott is approved:

Ross W Smith

Thesis Advisor

Department Chairman

Kenneth C. Kemp

Thesis Committee

John E Nellor

Dean, Graduate School

University of Nevada

Reno

May, 1983

ACKNOWLEDGMENTS

The author wishes to express his sincere gratitude to Dr. Ross Smith for the origination of the thesis topic and for his contributions and guidance throughout the entire investigation. He also expresses his appreciation to J. Chini and S. McGill for their contributions regarding this thesis.

The author also wishes to thank the National Science Foundation for funding this investigation under N.S.F. Grant ENG-7910010.

The author expresses special thanks to his wife, Jana, for her encouragement and help in editing this thesis.

ABSTRACT

The effects of mineral pretreatment, ionic strength, pretreatment temperature, and cationic collector type on the flotation characteristics of quartz and magnetite were investigated. The extent of crushing prior to pretreatment had a significant influence on quartz flotation recovery from approximately pH 2 to pH 8. Alkyl amine collector chain length and the presence of one or two functional amino groups were critical parameters related to ionic strength. Increasing the pretreatment temperature had a slight depressing effect on quartz and magnetite flotation recoveries. In most cases, n-dodecyl-1,3-diaminopropane was a superior flotation collector to n-dodecylamine for the recovery of quartz and magnetite.

TABLE OF CONTENTS

LIST OF FIGURES AND TABLES

TABLE

INTRODUCTION

Inorganic electrolytes are sometimes used as depressants and activators in the flotation of minerals. In amine flotation processes the effects of cations, particularly those ions found in sea water or ions which contribute to water hardness, can produce undesirable activation or depression in the flotation pulp. The use of calcium chloride to prevent freezing in ore cars, chutes and bins may be yet another source of salt contamination (Dayton, 1980). The salt(s) initially contained in the mill feed water may become more concentrated due to recycling of plant water. Recycling may be necessary because of environmental regulations or because of the unavailibility of water. In some cases, it may be desirable to use sea water rather than fresh water for the flotation fluid.

Many studies have been conducted on the presence of inorganic salts in flotation pulps, regarding their effects upon flotation recoveries and surface properties of different oxide minerals. It has been reported that the addition of an inorganic salt can increase or decrease flotation recoveries depending on the system (Somasundaran, 1975; Rajala, 1981; Fuerstenau and Modi, 1960; Kulkarni and Somasundaran, 1977). It has also been shown that the surface charge on oxide minerals can be reduced by the presence of a monovalent salt, whereas charge reversal is possible with the addition of a multivalent salt (Gaudin and Fuerstenau, 1955; Fuerstenau and Modi, 1959).

Even though considerable research has been conducted on the subject of ionic strength, information relating monoamine and diamine oxide flotation systems in high ionic strength pulps is scarce. A thorough study focusing on cationic collector systems in ionic strength pulps would further expand our understanding of such systems. Recently, an adsorption-flotation study has been completed. This study, discussion of which follows, relates variables that include monoamine and diamine collectors, collector chain length, pH's, monovalent and divalent salts, ionic strength, different oxide minerals, pre-conditioning temperature and pretreatment of the mineral(s) prior to flotation.

LIST OF NOMENCLATURE AND ABBREVIATIONS

12A	n-dodecylamine	$C_{12}H_{25}NH_2$
8D	n-octyl-1,3-diaminopropane	$C_8H_{17}NH(CH_2)_3NH_2$
12D	n-dodecyl-1,3-diaminopropane	$C_{12}H_{25}NH(CH_2)_3NH_2$
16D	n-hexadecyl-1,3-diaminopropane	$C_{16}H_{33}NH(CH_2)_3NH_2$
mV	Millivolts	
<u>M</u>	Moles per liter	
ml(s)	Milliliter(s)	
gm(s)	Gram(s)	
CMC	Critical micelle concentration	
PZC	Point of zero charge	
NaCl	Sodium chloride	
$CaCl_2$	Calcium chloride	
Na_2SO_4	Sodium sulfate	
HCl	Hydrochloric acid	
NaOH	Sodium hydroxide	

THEORETICAL CONSIDERATIONS

Unlike the adsorption of xanthates on galena, sulfonates, sulfates and alkyl amines are considered to adsorb on minerals primarily by electrostatic attraction. This is the result of the attraction between the polar head of the collector and the charged surface sites on the mineral. The attraction exhibited by the collector and mineral can be influenced by such variables as pH, type of salt(s) present, salt concentration, collector concentration, collector chain length, mineral pretreatment and temperature.

Theories dealing with mineral surface charge origin have been postulated by Parks, Healy and Fuerstenau (Parks, 1965; Healy and Fuerstenau, 1955), among other researchers. Simple oxides such as quartz and magnetite acquire a negative surface charge through reaction with water and dissociation of the surface hydroxides. As oxide minerals are ground to a certain size fraction for optimum flotation, bonds become broken. These broken bond surfaces can adsorb hydrogen and hydroxyl ions. This is followed by dissociation of the hydrated surfaces. Possible reactions illustrating this may be written as follows:

(1) $M)\text{-}OH = M)\text{-}O^{-} + H^{+}$

(2) $M)\text{-}OH + H^{+} + M)\text{-}OH_2^{+}$

M represents a metal and)- represents the species at the mineral surface. Equation (eq.) (1) shows the ionization of the hydrated surface. Eq. (2) shows the effect due to the addition of excess hydrogen ions. Therefore, hydrogen and hydroxyl ions are considered to be potential-determining ions. Surface charge origin may also involve the dissolution of the mineral and then readsorption of the complexes formed during hydrolysis of the dissolved material. For minerals such as quartz and magnetite, pH controls the extent of dissolution.

The potential-determining ions at the mineral-solution interface must maintain electroneutrality with the conditions prevailing in the system. In achieving this goal, a structure which surrounds the particle is produced. This structure is termed the electrical double layer. Figure 1 shows the double layer according to Stern. Region 1 contains the potential-determining ions which are regarded as part of the solid lattice. Region 2 consists of the counter-ions which are attached directly to the mineral surface in a layer called the Stern layer. This region is only a few angstroms in thickness. Region 3 consists of counter-ions which extend out into the bulk of the solution and form an atmosphere called the diffuse or Gouy layer. In this region, the ion concentration density decreases exponentially with the distance from the mineral surface.

The potential-determining ions give rise to the double layer. Counter-ions are drawn by electrostatic forces in order to maintain electroneutrality at the mineral-solution interface. The ions in the Stern layer are believed to be held at the mineral surface, whereas ions in the diffuse layer are able to move about freely.

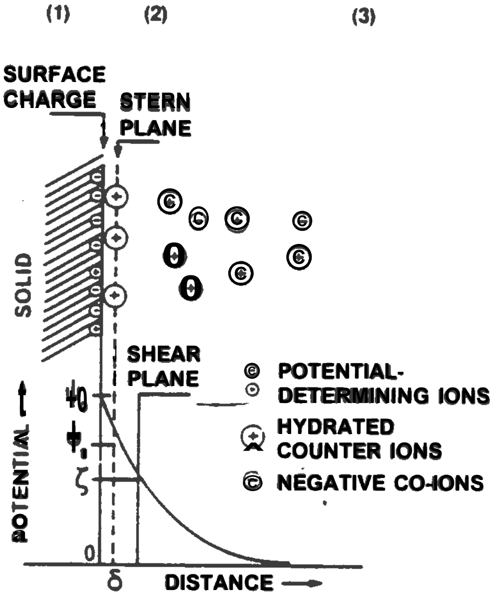

Fig. 1 Schematic representation of the structure of the double layer and potential in the double layer in electrolyte solutions (Stern's model).

The surface potential, Ψ_o , or the total potential across the double layer is determined by the concentration of potential-determining ions in solution only (Kruyt, 1952). Ψ_δ is the potential relative to the bulk of the solution at the center of charge in the Stern plane. δ represents the distance that the anchored layer of counter ions is from the surface. The electrical potential denoted at the shear plane-- (this plane is assumed to coincide with the boundary between the Stern and diffuse layers), is called the zeta potential (ζ).

The absolute value of the zeta potential (in mV) depends on Ψ_o , total electrolyte concentration, the location of the shear plane, and on the charge distribution. There are several methods for determining the zeta potential and they are well documented in the literature (Adamson, 1976).

Zeta potential studies are used extensively to describe electrokinetic properties of many minerals, particularly the simple oxides. The pH value at which a mineral has zero zeta potential is called the point of zero charge (PZC). Above the PZC, the mineral is negatively charged, whereas the mineral is positively charged below its PZC. The PZC for quartz is approximately 2, however, values up to 3.7 have been reported (Gaudin and Fuerstenau, 1955; Iwasaki, Cooke and Choi, 1961). The PZC for magnetite is 6.5 (Iwasaki, Cooke and Kim, 1962). The exact pH value at which the zeta potential is equal to zero is dependent on many variables, such as-- the history of the mineral, including the nature of the pretreatments that it has received, method of storing and aging, the extent of aging that takes place in an aqueous environment, mineral impurities, and pH. In regard to pretreatment, values reported for the zeta potential of quartz leached with different acids were quite different, depending on the leaching media used (Somasundaran, 1975). Similar observations have been noted for magnetite (Kolarik, Dixon, Freeman, Furlong and Healy, 1980).

Recently, it has been found that leaching quartz with hydrofluoric acid solution can raise the PZC of quartz from 2 to as high as 6 (Kulkarni and Somasundaran, 1972). However, upon aging the hydrofluoric acid-leached quartz in water, the PZC will return to its original value, but only over a period of several days.

Other possible differences noted in the PZC of a mineral may possibly be due to the method employed in measuring the zeta potential.

The zeta potential of a mineral can change with the addition of an inorganic salt (Gaudin and Fuerstenau, 1955). Monovalent salts such as sodium chloride can reduce the zeta potential of a mineral, however they will not reverse it. Salts such as sodium chloride have been termed indifferent electrolytes. Their ions have no special affinity for a mineral surface and function primarily as counter-ions in the double layer, whereas, given the presence of enough multivalent ions such as barium nitrate, which has opposite charge to the mineral surface, the zeta potential can be reversed. Multivalent ions such as barium and sulfate have been termed specifically adsorbed ions because they can produce zeta reversal. Zeta charge reversal is caused by the presence of more charge in the anchored layer than on the mineral surface. In other words, if counter-ions are specifically adsorbed, meaning that they have an affinity for the mineral surface, in addition to electrostatic attraction, then more ions can be adsorbed than there are surface charges available, and the sign of the zeta potential can be reversed even though Ψ_o remains constant.

Zeta reversal can also occur due to polyvalent metal ions which have formed their first hydroxy complex through hydrolysis (Fuerstenau and Palmer, 1976).

The first hydroxy complex functions as a modifier. The modifier can be an activator or a depressant, depending on the type of collector used, mineral PZC, etc. Hydroxy complexes are such surface active substances that they have been reported to adsorb on positively charged surfaces. The adsorption of a hydroxy complex could adversely affect the cationic flotation of oxide minerals (Smith and Akhtar, 1976).

Historically, the most commonly used cationic collectors (surfactants) in flotation are the acetate and chloride salts of n-dodecylamine (Ralston, 1948). It has been general practice for many years in the benificiation of metal oxides containing quartz, to float the silica using the above-mentioned collectors. This is primarily for two reasons: 1) the dodecyl chain length is sufficiently long enough to render the quartz surface hydrophobic at low collector concentrations, and 2) the dodecylamine salts are readily soluble. A group of cationic collectors which is finding wide acceptance in the flotation field is the cationic diamines.

These compounds have two functional amino groups, and are found to be more efficient than corresponding monoamines for many systems (Bleir, Goddard and Kulkarni, 1976).

Dodecylammonium ions in dilute solutions are adsorbed as individual ions and are considered to function primarily as counter-ions (Bruyn, 1955; Gaudin and Morrow, 1954). However, once the adsorbed dodecylammonium ions reach a certain concentration at the mineral-solution interface, the collector ions begin to show a special affinity for the mineral surface. This is illustrated by the fact that zeta reversal occurs along with a marked increase in collector adsorption, contact angle and flotation recovery (Fuerstenau, Healy and Somasundaran, 1964), at amine concentrations greater than a certain amount. As the total amine concentration in the electrical double layer is increased, a certain critical value is reached. At this value, adsorption occurs via association of hydrocarbon chains. This phenomenon is analogous to the formation of micelles in solution at the critical micelle concentration (CMC), and therefore has been termed hemimicelle formation (Gaudin and Fuerstenau, 1955).

The CMC of a collector is defined as the bulk concentration at which micelles begin to form. Micelles can be considered as colloidal-size aggregates of organic ions which have their non-polar chains removed from water by tight association of the chains inward, with the polar heads oriented outward toward the water (solution). The characteristics of a micelle, e.g., shape and size, are determined by the equilibrium between the repulsive forces of the polar charged heads and the attractive forces of the non-polar hydrocarbon chains. The CMC at which micelles form depends upon the number of carbon atoms in the hydrocarbon chain. The CMC increases slightly with increased temperature, but dependence is not great.

The CMC of a collector can be lowered by the addition of an inorganic salt. This may result in the formation of micelles in the bulk solution. This would decrease the amount of amine available for adsorption and thus affect flotation recovery.

Hemimicelle formation is attributed to a free energy decrease, which is caused by the removal of hydrocarbon chains from the aqueous media. The free energy decrease associated with hemimicelle formation has been determined to be about 1.1 kT per CH_2 group, where k is the Boltzmann constant and T is the absolute temperature (Fuerstenau, Healy and Somasundaran, 1964; Stigter and Overbeek, 1958).

Adsorption of cationic collectors in the Stern layer is then the result of electrostatic attraction and another force resulting from the free energy decrease associated with the removal of the hydrocarbon chains from water. Neutral molecules may also be incorporated in the formation of hemimicelles. The adsorption of a collector onto a mineral surface when hemimicelle formation occurs is given by the following relation (Smith and Akhtar, 1976):

$$(3) \quad \Gamma_1 = 2r_1n_1 \exp - \frac{(ve\zeta + \lambda p + a\phi)}{kT}$$

Where:

Γ_i = adsorption density of the collector (ions per cm^2)
r_i = radius of the head of the adsorbing ion in cm
n_i = number of collector ions per cc in bulk solution
v = valency of adsorbing ion
e = electronic charge
ζ = zeta potential in mV
λp = contribution to adsorption not attributable to electrostatic interaction or to association of hydrocarbon chains
a = number of carbon atoms in alkyl chain
ϕ = work of adsorption for each CH_2 group that results from association of hydrocarbon chains approximately 1.1 kT
k = Boltzmann's constant
T = absolute temperature, $^{\circ}K$

If one considers an 8 carbon collector with no hemimicelle formation, then the $a\phi$ term would be zero. However, when the collector ions and possibly neutral molecules are adsorbing as hemimicelles, the $a\phi$ term should approach 8 kT as monolayer coverage on the substrate is approached. It is possible to deduce from eq. (3) that collector adsorption is also dependent on chain length. Thus, flotation recovery may be enhanced by longer-chained collectors due to an increase in adsorption density as compared with shorter-chained collectors. However, as collector chain length is increased, solubility decreases and frothing characteristics increase. Once the amine concentration reaches a value where the full adsorption potential is effective, the addition of inorganic salts has no effect on the flotation recovery of quartz for the systems studied (Onoda and Fuerstenau, 1964). However, when amine concentration is kept constant and inorganic salt concentration increased, flotation recovery drops off accordingly.

The specific adsorption potential can be determined in a number of ways. One way is to treat the double layer as a molecular condenser when the zeta potential is zero (Fuerstenau, 1962).

Dodecylammonium ions appear to be adsorbed electrostatically below about 10^{-4} M at neutral pH, however, as surfactant ions crowd into the Stern layer, they begin to associate through their hydrocarbon chains. Between 10^{-4} and 10^{-3} M approximately, the specific adsorption potential increases from about zero to a maximum of about 12 kT (8 kcal per mole). This is considered to be the maximum energy that can be gained by the removal of a 12-carbon chain from water. Once the dodecylammonium acetate concentration is increased above 5×10^{-4} M, the specific adsorption potential becomes effective and surfactant ions are preferentially adsorbed.

For particulate flotation, an excess amount of collector can reduce flotation recovery by causing a size reduction of the bubbles to such an extent that they are not capable of levitating the mineral particles that collect on them (Somasundaran and Kulkarni, 1973); adsorption of a second layer of collector species with an orientation opposite the first layer, or adsorption as micelles may also occur.

The following expression (Shinoda, 1963) relates the critical micelle concentration of a homologous series of collectors to electrolyte strength and is given by the relation:

$$(4)\quad \ln \mathrm{CMC} = -\frac{MW}{kT} - (K_g)\ln C_i + K_1$$

where

M = the number of methylene groups in the hydrocarbon chain

W = the standard free energy change per methylene group upon micellization, about 1.1 kT

K_g & K_1 = constants for a specific homologous series of collectors

C_i = total concentration of counter-ions

Equation (4) suggests that a longer-chained cationic collector in a homologous series will have a lower CMC than a shorter-chained collector in the presence of an equivalent amount of salt. Furthermore, the addition of a divalent salt such as calcium chloride or sodium sulfate should lower the CMC even more compared to an equivalent addition of a monovalent salt, e.g., sodium chloride, due to the increase in charge or ionic strength. Table 1 shows critical micelle concentrations of some selected amines at approximately 22°C (Smith and Chini, 1980). It can be seen from Table 1 that an increase in collector chain length, or an increase in ionic strength lowers the CMC. Therefore, a shorter-chained collector may give better flotation results in the presence of salts, due to the presence of more available

TABLE 1

Critical micelle concentrations for
some selected amines (22 ± 1°C)

Surfactant	CMC In pure water	 In 0.6M NaCl	 In 0.1M $CaCl_2$
n-octylamine	5.0×10^{-2}	-	-
n-dodecylamine	1.2×10^{-2}	-	-
n-tetradecylamine	2.5×10^{-2}	-	-
n-hexadecylamine	7.5×10^{-2}	-	-
n-octadecylamine	4×10^{-4}	-	-
n-octyl-1,3-diaminopropane	6×10^{-2}	2.5×10^{-2}	1.5×10^{-2}
n-dodecyl-1,3-diaminopropane	1.5×10^{-2}	2×10^{-3}	5.5×10^{-3}
n-hexadecyl-1,3-diaminopropane	1.0×10^{-3}	2.5×10^{-4}	2.5×10^{-4}
n-octadecyl-1,3-diaminopropane	1.5×10^{-4}	-	7×10^{-5}

amine in the ionic form as compared with the longer-chained amines.

For flotation to occur in oxide mineral systems, an appreciable amount of collector must be present in the ionic form. In the case of n-dodecylamine and n-dodecyl-1,3-diaminopropane (the former being a stronger base than the latter), the dissociation constants are important because they determine the proportion of neutral molecules to ionic species in the system. The pKa value of the substance is the value at which the molecular and ionic species are equal in concentration. Flotation at this value may be beneficial since it promotes stronger adsorption, and in many systems, flotation recovery is at a maximum (Smith and Akhtar, 1976). The reason for this is that there is a more uniform distribution of the collector on the mineral surface as opposed to a situation where the concentration of the ionic species is high. By considering dissociation constants for an amine in an aqueous environment, it is possible to construct a log concentration diagram which shows the concentration of the various species as a function of pH. If dissociation constants are considered for reactions of the type:

(5) $C_{12}H_{25}NH_2(aq) + H_2O = C_{12}H_{25}NH_3^+ + OH^-$

(6) $C_{12}H_{25}NH(CH_2)_3NH_2(aq) + H_2O = C_{12}H_{25}NH(CH_2)_3NH_3^+ + OH^-$

$C_{12}H_{25}NH(CH_2)_3NH_3^+ + H_2O = C_{12}H_{25}NH_2^+(CH_2)_3NH_3^+ + OH^-$,

curves such as those noted in Figures 2 and 3 may be constructed. Figure 2 shows a log concentration diagram for

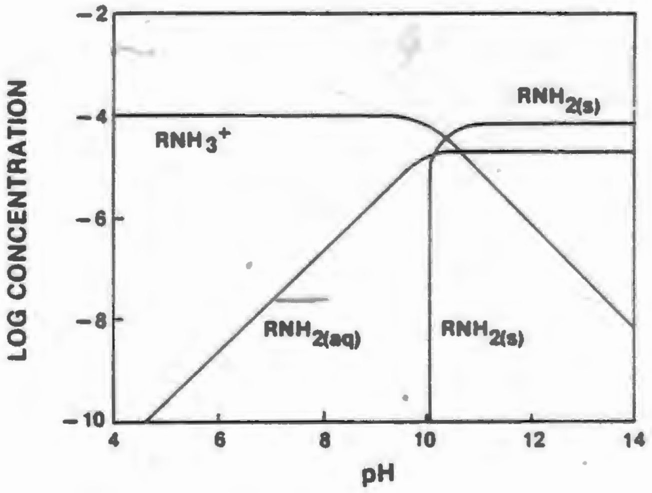

Figure 2. Logarithmic concentration diagram for 1 x 10^{-4} M total n-dodecylamine.

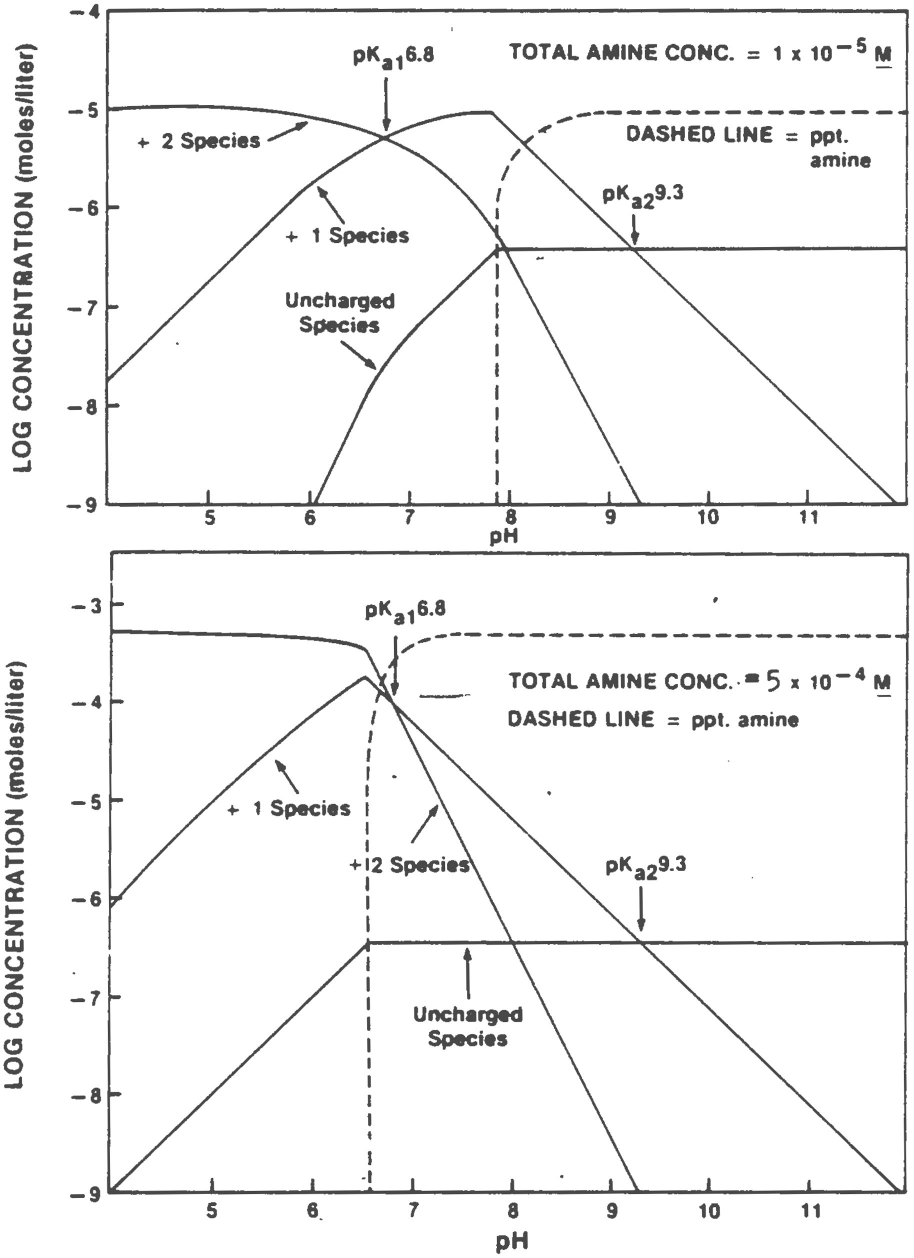

Figure 3. Log concentration diagrams for 1 x 10^{-5} M and 5 x 10^{-4} M Total concentration Duomeen 120.

n-dodecylamine at 10^{-4} M total concentration (Smith and Akhtar, 1976). Figure 3 shows a log concentration diagram for n-dodecyl-1,3-diaminopropane at 10^{-5} M and 5×10^{-4} M total concentrations (Smith and McGill, 1981). From Figures 2 and 3 it can be seen that pH substantially changes the form of n-dodecylamine and n-dodecyl-1,3-diaminopropane in solution. Figure 2 shows that RNH_3^+ is the predominating species at pH values less than approximately pH 7. At pH 10.65 (pKa value) the concentrations of ionic and nonionic species are equal, with the quantity of RNH_3^+ dropping off above the precipitation of $RNH_2(s)$. Figure 3 shows a similar relationship, except two ionic species are present. At pKa_1, the two ionic species are equal in concentration, however, above this value the +1 species predominates. At pKa_2, the uncharged and +1 species are equal in concentration.

Comparing Figures 2 and 3, despite differences in total collector concentration, flotation behavior exhibited by a monoamine versus a diamine mineral system, would be expected to differ.

The concentrations of different ions in the double layer will depend primarily on their valence, specific adsorption potential and bulk concentration. The concentrations of ions at any point in the double layer can be calculated by use of Boltzmann's relation, provided electrokinetic data is available (Gaudin and Fuerstenau, 1955). When the adsorbed collector ions are not associated (below hemimicelle formation) in the double layer, it is possible to quantitatively determine the effectiveness of inorganic ions on the depressing effect exhibited in flotation systems by the following relation (Aplan and Fuerstenau, 1962):

$$(7) \qquad \frac{\Gamma a}{\Gamma b} = \frac{C_a}{C_b} \exp \frac{\phi_a - \phi_b}{kT}$$

where

Γa & Γb = adsorption densities of ions a and b

C_a & C_b = bulk concentrations of ions a and b

ϕ_a & ϕ_b = adsorption potentials of ions a and b

The following is a brief summary of oxide flotation principles:

1) Flotation of oxide minerals often depends on the electrostatic interaction between the mineral and collector.

2) The effect of pH can change the mineral's surface electrical potential. It also influences the extent of collector hydrolysis.

3) Pretreatment conditions of a mineral can change its PZC.

4) Inorganic ions compete with collector ions for charged sites on the mineral surface, and thus reduce collector adsorption.

5) For significant adsorption to occur, according to the hemimicelle theory, the mineral surface should be negatively charged so that the critical hemimicelle concentration is reached before the CMC in the bulk solution.

6) As collector chain length is increased, solubility

decreases, frothing power increases and the CMC is lowered. This lowers the quantity of collector required for hemimicelle formation.

7) Collector adsorption is related to the free energy decrease associated with the expulsion of each CH_2 group from the solution by association of hydrocarbon chains.

8) A moderate collector concentration is usually required.

9) Conditioning time prior to flotation is generally short.

10) Collector-mineral attachment appears not to be very strong.

11) Multivalent anions, such as SO_4^{2-}, can adsorb on a mineral below its PZC and thus promote adsorption of a cationic collector.

EXPERIMENTAL

Minerals and Their Pretreatment

The minerals considered for this investigation were quartz and magnetite. The quartz was obtained from Hot Springs, Arkansas, the magnetite from Ishpeming, Michigan. Both were purchased from Ward's Natural Science Establishment. Table 2 shows the spectrographic analysis of the minerals obtained from Ward's.

The size fraction used for quartz and magnetite adsorption studies was -65 +325 mesh. The size fraction used in the microflotation studies was **-65** +150 mesh. This size fraction should reflect flotation rates relative to other systems.

High purity quartz crystals were crushed and then ground by hand with a mortar and pestle. This material was hand screened to the desired size fraction, and then ro-tapped for 30 minutes. After dry screening, the quartz samples were leached in concentrated HCl, which was brought to boiling for a total time of 5 minutes, and then allowed to stand for 10 minutes. Afterwards, the sample was rinsed with double-distilled water until the pH of the rinse water was that of the double-distilled water alone. This was followed by wet screening 5 times in double-distilled water. The sample was then oven-dried at approximately **95°C**.

TABLE 2

Spectrographic analysis of quartz and magnetite

QUARTZ

Metal	Percentage
Ag	<0.001
Al	0.1
Cr	0.005
Cu	0.007
Fe	0.007
Mg	<0.001
Ni	0.02
Pb	<0.01
Si	Major
Ti	0.002

MAGNETITE

Metal	Percentage
Al	2.0
B	0.04
Cu	<0.001
Fe	Major
Mg	0.1
Mn	0.05
Na	0.4
Pb	0.2
Si	1.0

Variations in leaching time, HCl concentration and extent of crushing prior to leaching were performed on some quartz micro-flotation feed samples. The importance of this will be discussed where applicable.

Magnetite samples were prepared by first crushing in a clean laboratory jaw crusher. The crushed magnetite was then ground by hand with a mortar and pestle. This material was hand screened to the desired size fraction. The sample was then ro-tapped for 30 minutes. After dry screening, the magnetite samples were leached in a 0.1 M HCl solution, which was brought to boiling and then allowed to stand for 15 minutes. After this, the sample was rinsed with double-distilled water, wet screened and then oven-dried at approximately 95°C in the same manner as noted for quartz.

Reagents

The diamine compounds Duomeen 8D, 12D, 16D and 16 were obtained from Armac Co., McCook, Illinois. The Duomeens 8D, 12D and 16D were greater than 90 percent pure. Also obtained from Armac was Armeen 12D (12A), which also was greater than 90 percent pure.

Reagent grade glacial acetic acid was used to convert the 8D, 12D, 16D, 16 and 12A amine compounds to the acetate salt form.

The inorganic salts studied included reagent grade sodium chloride, anhydrous calcium chloride, and sodium sulfate.

Reagent grade sodium hydroxide and hydrochloric acid were used as pH modifiers.

The reagents used in the colorimetric adsorption procedure included reagent grade chloroform and picric acid.

All solutions were prepared with double-distilled water.

Salt Concentrations

NaCl, $CaCl_2$, and Na_2SO_4 concentrations were kept constant in adsorption and microflotation studies, while collector concentrations were varied. These salts should show the effects of positively- and negatively-charged monovalent and divalent ions on the adsorption and microflotation of quartz and magnetite.

The salt concentrations were 0.6 $\underline{M}$ NaCl, 0.1 $\underline{M}$ $CaCl_2$, and 0.1 $\underline{M}$ Na_2SO_4. In the case of NaCl, the salt concentration was that of sea water. The concentrations of the divalent salts studied are possible for some systems.

Collector Preparations

Monoamine collector solutions were prepared by adding a known weight of amine to a volumetric flask and then filling with double-distilled water to about one-fourth full. A one-to-one equivalent weight of glacial acetic acid was then added and the flask was transferred to a hot plate stirrer and gradually heated to approximately 45°C. As the primary amine (12A) dissolved, more water was added in 200 ml increments until the flask could be held up to the light and no particles or cloudiness appeared. The collector solution was then cooled to 25°C and brought to volume. The same procedure was performed for the diamine compounds, except a two-to-one equivalent weight of glacial acetic acid was added. Collector solutions were prepared daily.

Preparation of the collectors in salt solutions resulted in precipitation of the collectors. To prevent this, the collector solutions were first prepared, then the desired weight of salt was added. The flask was then returned to the magnetic stirrer until the salt was dissolved.

Collector concentrations ranged from 1×10^{-3} M to 1×10^{-6} M.

Adsorption Studies

Collector adsorption of 12D on quartz and magnetite was investigated using the colorimetric Picric Acid Method (Li, 1957). Results of these studies should provide some correlation between possible collector adsorption mechanisms and microflotation results.

Using the Picric Acid Method, equal amounts of the amine solution and a 0.2% solution of picric acid in chloroform were mixed together and then allowed to separate. The amine picrate that was formed went into the chloroform phase and the remaining picric acid went into the water phase. Once the two phases separated, the chloroform was extracted and read colorimetrically at 410 nanometers. A description of the lab procedure follows.

Before adsorption studies were begun, a calibration curve was constructed. This was done by adding 10 mls of collector solution ($25^{\circ}C$) of known concentration into a separatory funnel in which 10 mls of the 0.2% picric acid chloroform solution were added. The phases in the separatory funnel were then mixed by rotating the funnel through a 180 degree arc 100 times. The mixture inside the funnel was then allowed to stand for 5 minutes, at which time the organic phase was removed and read at 410 nanometers in a Baush and Lomb spectrophotometer. This resulted in values of absorbance versus a known collector concentration. A linear calibration curve was then plotted. This plot was used for determining unknown collector concentrations from absorbance measurements. The procedure for determining adsorption of 12D onto quartz and magnetite follows.

For each test, a one gram sample of the mineral was placed in a 100 ml beaker, to which 20 mls of collector solution were added. Next, 20 mls of collector solution were added to another 100 ml beaker containing no mineral. For both samples the initial pH was taken and then adjusted with HCl or NaOH in the range pH 2 to pH 12. Both beakers were then covered with parafilm and placed in a circular rotating water bath at 60 rpm, for 5 minutes at $25^{\circ}C$. The samples were then removed and final pH values read. 10 mls of collector solution from the mineral-containing beaker were pipetted into a separatory funnel. 10 mls of the picric acid chloroform solution were then added to each funnel and mixed as noted previously. The samples were then allowed to stand for 5 minutes before extracting the organic phase and reading at 410 nanometers on the spectrophotometer. The values obtained for absorbance were then compared with the calibration curve to determine collector concentration. Next, the concentration obtained for the sample containing mineral was subtracted from the concentration of the blank. The resulting concentration was then used to calculate adsorption per gram mineral. The following example shows how adsorption per gram mineral was calculated.

	Absorbance	Concentration (moles/liter)
Blank	0.298	4.4 x 10^{-4}
Sample	0.290	4.2 x 10^{-4}

Blank concentration minus sample concentration equals 0.2 x 10^{-4} M. (0.2 x 10^{-4} moles/liter) x (20 mls/gm sample) x (1 liter/1000 mls) = 4.0 x 10^{-7} moles of adsorbed collector per gram sample. This is generally reported as 4.0 x 10^{+7} moles of adsorbed collector per gram sample. Results in the following section will be reported in this fashion.

Regarding magnetite adsorption studies, a slight modification was necessary. Initially, all 12D 10^{-5} M adsorption results for magnetite were negative. This is theoretically impossible. It was found that by preparing a magnetite sample containing double-distilled water only, in conjunction with the other two samples, and following the same procedure as noted above, that absorbance interference, presumably due to the oxidation of Fe^{2+}, could be resolved. The absorbance reading was then either subtracted from blank absorbance or added to sample absorbance readings. In either case, the calculated concentration was the same. Adsorption per gram mineral was then calculated as noted above.

Microflotation Studies

Results of these studies should illustrate the differences between collector chain length, and number of amino groups present, and give a positive correlation regarding adsorption studies under ionic strength conditions.

Figure 4 shows a schematic representation of the microflotation device. Microflotation studies were conducted in a Hallimond tube flotation cell. A description of the laboratory procedure for flotation studies follows.

For each microflotation test, the stopcock valves 4 and 6 were first positioned to allow N_2 gas flow. Next, the gas regulator valve (2) was adjusted to 8 psi. The N_2 gas then passed through a saturated NaOH solution (3), which removed CO_2 gas. The pressure created in the system caused the double-distilled water in the 100 ml buret to be forced into the head tank (7), thus filling the buret with cleaned N_2 gas. Once the water in the buret reached the 0 ml mark, valves 6 and 2 were closed. Stopcock 4 was then positioned so as to allow N_2 gas, created by pressure from the head tank, to flow from the buret into the flotation cell (8). Exactly

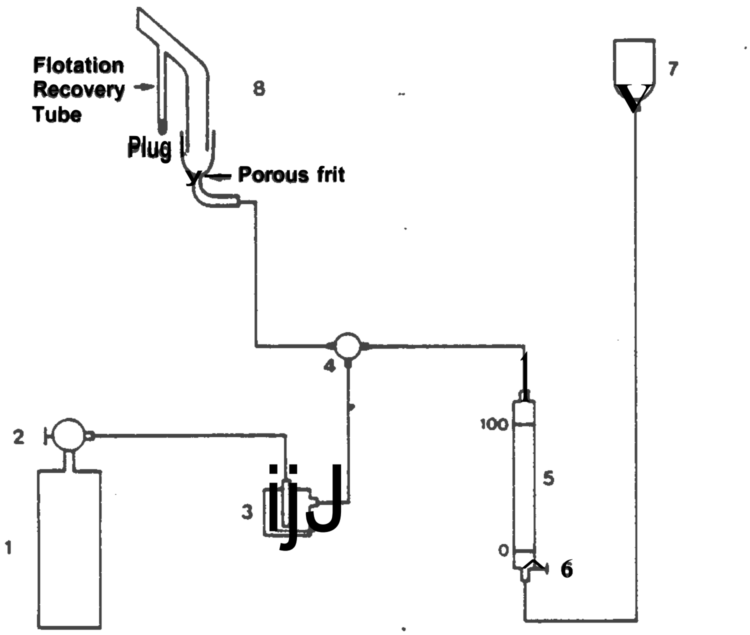

1. Nitrogen gas tank
2. Pressure regulator
3. Gas cleaning bottle
4. 3-way stopcock
5. 100 ml buret
6. Buret valve
7. Head tank
8. Hallimond tube

Figure 4. Schematic representative of the microflotation device.

100 mls of gas were passed through the flotation cell at a flow rate of 100 mls per 50 seconds.

The treated -65 +150 mesh size fractions of quartz and magnetite were used as the microflotation feed material. Flotation pulps were prepared by adding approximately 1 gram of quartz or magnetite to a 250 ml beaker, to which 170 mls of collector only, or collector-salt solution were added. The initial pH value was read and then adjusted to the desired value prior to the conditioning phase.

Conditioning for the two minerals was conducted at 25°C, 35°C and 75°C.

Flotation pulps conditioned at 25°C and 35°C were placed in a circular rotating water bath set at the desired temperature, at 60 rpm for 5 minutes. The final pH value was then recorded and the sample was transferred to a glass funnel which was plugged with a tapered rubber stopper attached to a glass rod. The pulp was then transferred to the microflotation cell via the glass funnel. After a total conditioning time of seven minutes, flotation was initiated.

Pulps conditioned at 75°C were heated on a bunsen burner until the desired temperature was reached. The temperature was then reduced to 25°C by holding the container under a running stream of cold water. The final pH was then recorded. After a total conditioning time of 12 minutes, flotation was initiated.

After flotation, the flotable portion of the mineral particles contained in the froth overflow and in the flotation recovery tube were collected. Then the non-flotable mineral particles which were left in the lower portion of the cell were collected. Both products were filtered, dried and then weighed. Percent flotation recovery was determined by dividing the flotable product weight by the total sample weight and multiplying by 100.

The lower portion of the Hallimond tube was specifically designed with sloping sides down to the glass porous frit in order to facilitate bubble-mineral contact. To further aid bubble-mineral contact, a light finger-tapping was provided at the lower portion of the flotation cell, near the glass porous frit. A modified Hallimond tube equipped with a magnetic stirrer could not be used in magnetite flotation studies, and so was not considered.

RESULTS

The results on the following pages are a compilation of the data obtained over a two-year investigation.

Figures 5 through 9 show the effects of conditioning rpm and sample size on quartz and magnetite adsorption studies.

Figures 10 through 13 illustrate the importance of quartz mineral pretreatment in regard to adsorption and flotation studies.

Figure 14 shows the effect of Duomeen 16 compound purity on the flotation recovery of quartz.

Figures 15 through 25 show the effects of ionic strength and temperature on the flotation recovery of quartz and magnetite using the Armeen and Duomeen compounds at 10^{-5} $\underline{M}$ and 10^{-4} $\underline{M}$.

Figures 26a through 33b are a compilation of some of the graphs found in Figures 15a through 25b. These figures show the effects of ionic strength, collector chain length and the number of amino groups present on the flotation recovery of quartz and magnetite in relation to the various amine compounds studied.

Experimental conditions different from those noted in the experimental section can be found on each figure or will be discussed where applicable.

Mineral pretreatment conditions were varied in some cases, but the comminution, rinsing, screening, leaching and drying procedures were conducted as noted in the experimental section.

Following is an individual description of the results obtained for Figures 5 through 33b.

The Effects of Conditioning RPM and Experimental Sample Size on the Adsorption of Duomeen 8D and 12D on Quartz as a Function of pH

Figure 5 shows initial adsorption studies of 10^{-4} $\underline{M}$ 8D and 10^{-4} $\underline{M}$ 12D on quartz as a function of pH in the presence of collector solution only. As can be seen, a large degree of scatter is apparent. This will be shown to be primarily due to conditioning rpm and experimental sample size (180 rpm, 0.2 gm sample). This type of behavior reflects the sensitivity of amine adsorption on quartz.

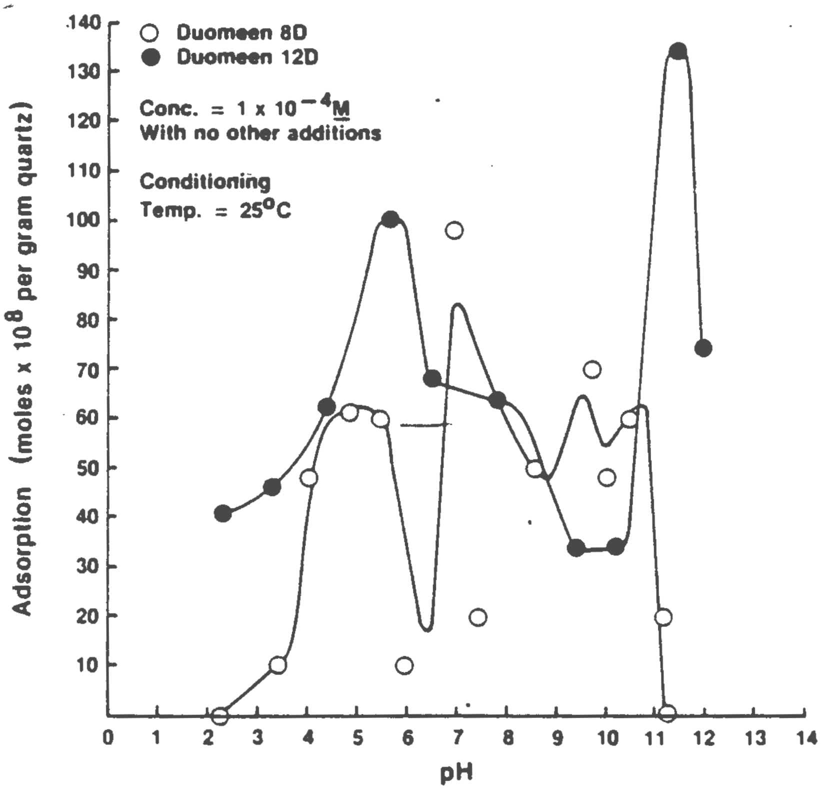

Figure 5. Adsorption of Duomeen 8D and 12D on quartz as a function of pH (180 rpm, 0.2 gm sample).

The Effect of Conditioning RPM on the Adsorption of 10^{-4} M 12D on Quartz in the Presence of Collector Solution Only

Figure 6 shows the effect of conditioning rpm on the adsorption of 10^{-4} M 12D on quartz in the presence of collector solution only at approximately pH 10, using a 0.2 gm experimental sample size. As can be seen, as conditioning rpm is increased, adsorption is decreased, with the exception at 60 rpm. Because 12D adsorption is seen to be greater at 60 rpm, all remaining adsorption and flotation experiments were carried out at this conditioning speed.

This increase in 12D adsorption at 60 rpm is believed to be the result of greater attachment and dispersion of the 12D collector within the electrical double layer. Because physical adsorption systems ~~have~~ reported bond energies less than 10 Kcal/mole, an increase in conditioning rpm results in greater shear forces at the electrical double layer-shear plane interface. This can cause a decrease in collector adsorption, which in turn, can influence a mineral's flotation recovery.

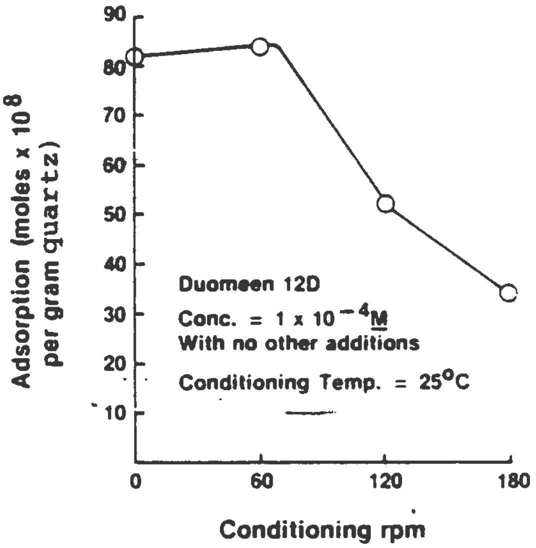

Figure 6. Adsorption of Duomeen 12D on quartz as a function of conditioning rpm, (pH 10.0 ± 0.22, 0.2 gm sample.)

The Flotation Recovery and Adsorption of 10^{-4} M 12D on Magnetite in the Presence of Collector Solution Only

Figure 7 relates zeta potential of acid/alkali pretreated magnetite to flotation recovery and adsorption of 10^{-4} M 12D as a function of pH in the presence of collector solution only.

The dashed line representing the zeta potential of magnetite was approximated using the Helmholtz-Smoluchowski approximation (12.8 EM = ζ mv) based on the work of Kolarik, Dixon, Freeman, Furlong and Healy (Kolarik, Dixon, Freeman, Furlong and Healy, 1980). These researchers have shown that differing magnetite pretreatments can have a pronounced effect on the electrokinetic properties of a natural magnetite. As will be seen in the case of quartz, not only do differing pretreatments affect its flotation characteristics, but the extent of crushing prior to pretreatment may adversely affect its flotation rate. This is quite interesting since it has never been shown before, to the author's knowledge.

The PZC of the magnetite mentioned above is 6.7. Adsorption experiments were not done as noted in the experimental section for magnetite. These tests were run as noted for quartz, without the additional water-magnetite sample. Also note that the adsorption study experimental sample size was 0.2 gm. It can be seen that the three curves correlate quite well after about pH 6. Once the magnetite surface becomes negatively charged, an increase in 12D adsorption is seen, with an increase in flotation recovery reaching

100 percent from about pH 9.5 to pH 11.5. Comparing Figures 5 and 7 for the 10^{-4} $\underline{M}$ 12D curves, it can be seen that 12D adsorption occurs extensively at or below their reported PZC's. The reason for this behavior is not clear. However, as will be seen in some of the following figures, once the experimental sample size is increased to 1.0 gram, a better correlation between adsorption and flotation recovery is observed for both quartz and magnetite.

Kolarik and co-workers have shown that warm or hot HCl acid pretreatment of magnetite shifts the mineral's PZC towards the higher pH range. This should be reflected by a decrease in 12D collector adsorption in the lower pH range, due to an increase in the positive surface charge of magnetite below its PZC. As can be seen from Figure 7, this type of behavior is seen for magnetite flotation recovery only.

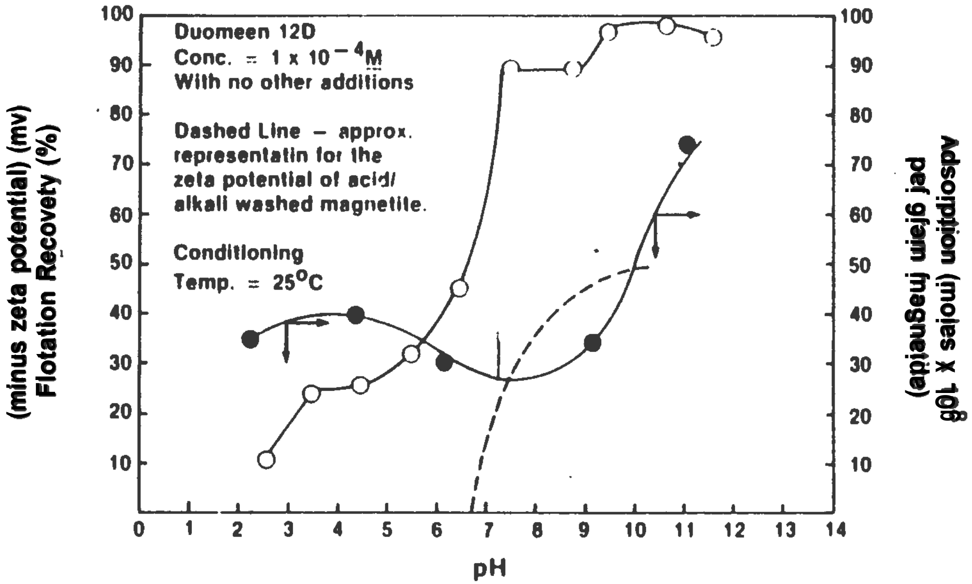

Figure 7. Zeta potential, flotation recovery and adsorption of Duomeen 12D on magnetite as a function of pH (60 rpm, 0.2 gram sample).

Adsorption of 12D on Quartz as a Function of Unadsorbed 12D in the Presence of Collector Solution Only

Figure 8 shows the effect of increasing 12D concentration in regard to adsorption on quartz in the presence of collector solution only, at approximately pH 8.5. It can be seen that as 12D concentration is increased, adsorption of 12D increases with the exception at 5×10^{-5} M 12D and 5×10^{-4} M 12D, where a slight decrease is observed. This is attributed in part to the 0.2 gm sample size and the variance of 12D adsorption occuring in this pH area, as will be seen in some of the following figures.

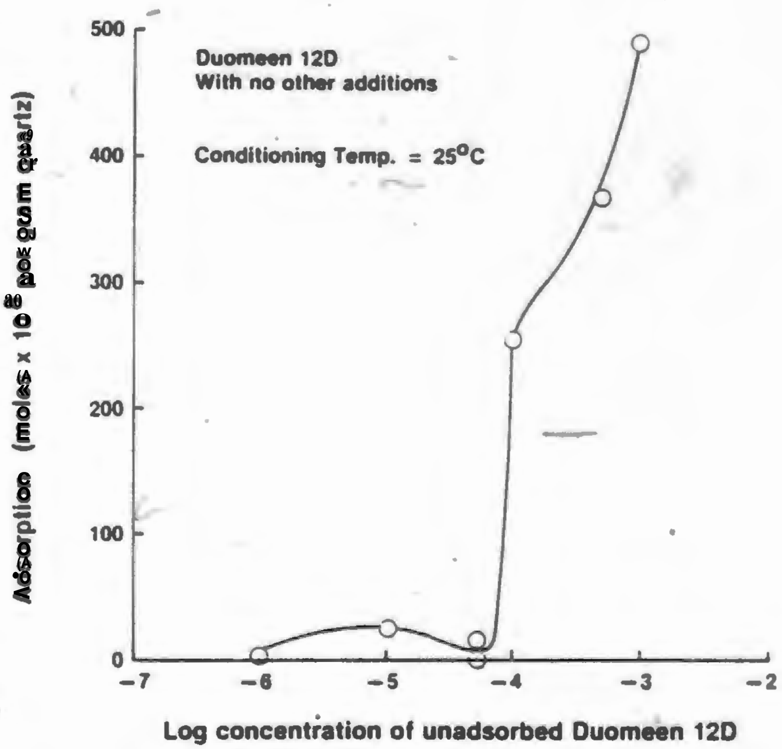

Figure 8. Adsorption of Duomeen 12D as a function of the log concentration of unadsorbed (final concentration) 12D on quartz at pH 8.5 ± 0.3 (60 rpm, 0.2 gm sample).

The Effect of Experimental Sample Size on the Adsorption of 5×10^{-4} M 12D on Quartz in the Presence of Collector Solution Only

Figure 9 shows the effect of pH on the adsorption of 5×10^{-4} M 12D on 0.2 and 1.0 gram quartz samples in the presence of collector solution only, as a function of pH. Notice the degree of scatter and the increase in adsorption in the lower pH range for the 0.2 gram sample curve. As can be seen, the 1.0 gram sample curve gives consistent results. This curve is reproduced in Figure 11b.

The occurrence of the two adsorption peaks in the lower and higher pH ranges is attributed to the additional amino group. For quartz primary amine adsorption systems, the existence of the first peak from approximately pH 5 to pH 6 has never been seen. Recall Figures 2 and 3. Comparing the pKa values for the 5×10^{-4} Log Concentration curve and the adsorption peaks found in Figures 9 and 11b, it can be seen that the pKa values correspond closely with the two noted adsorption peaks. This type of behavior for diamine systems has never been shown before. The first adsorption peak is shifted slightly to the left of pKa_1, whereas, pKa_2 corresponds to the adsorption peak at pH 9.5 almost perfectly.

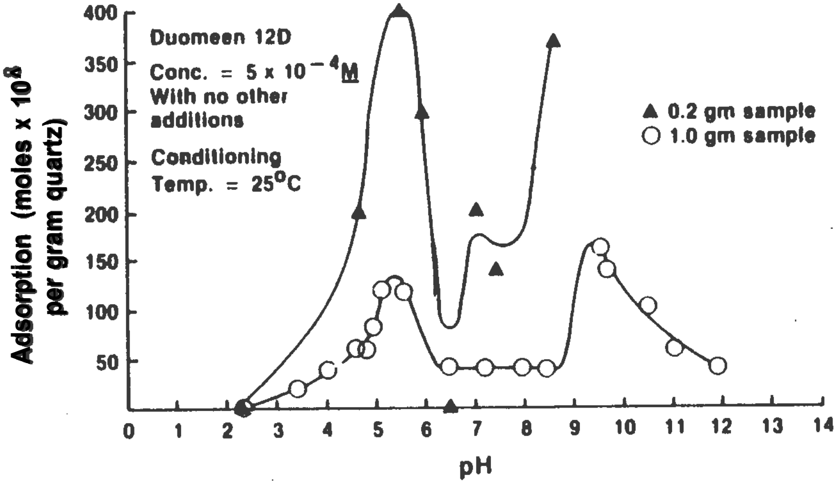

Figure 9. Adsorption of Duomeen 12D on quartz as a function of pH (60 rpm).

The Effect of Quartz Pretreatment on Flotation Recovery Using 10^{-5} M and 10^{-4} M 12D in the Presence of Collector Solution Only

Figures 10a and 10b show the effects of pH, pretreatment and flotation recovery of quartz in the presence of collector solution only.

The quartz samples used for the 10^{-5} M 12D open circle curve in Fig. 10a were crushed to -65 +150 mesh, stored in double-distilled water for 24 hours, wet screened and then oven-dried at 95°C.

The quartz samples used for the 10^{-5} M closed circle curve in Figure 10a were obtained from a graduate student who worked on this investigation prior to myself. The precise pretreatment conditions are unknown, but are believed to be as follows:

Quartz crystals were first slightly broken up, and then leached in hot HCl for 15 minutes, and dried. The broken up crystals were then crushed to -65 +150 mesh. The HCl leach concentration and the temperature of drying are unknown. As can be seen, this curve lies between the open circle and the open square 10^{-5} M curves in the lower pH range. This curve is reproduced in Figure 11a (open square).

The quartz samples used for the 10^{-5} M 12D open square curve in Figure 10a were prepared as follows:

Quartz crystals were first leached in concentrated boiling HCl for 15 minutes, rinsed, dried, crushed to -65 +150 mesh, wet screened and then oven-dried at 95°C. The quartz

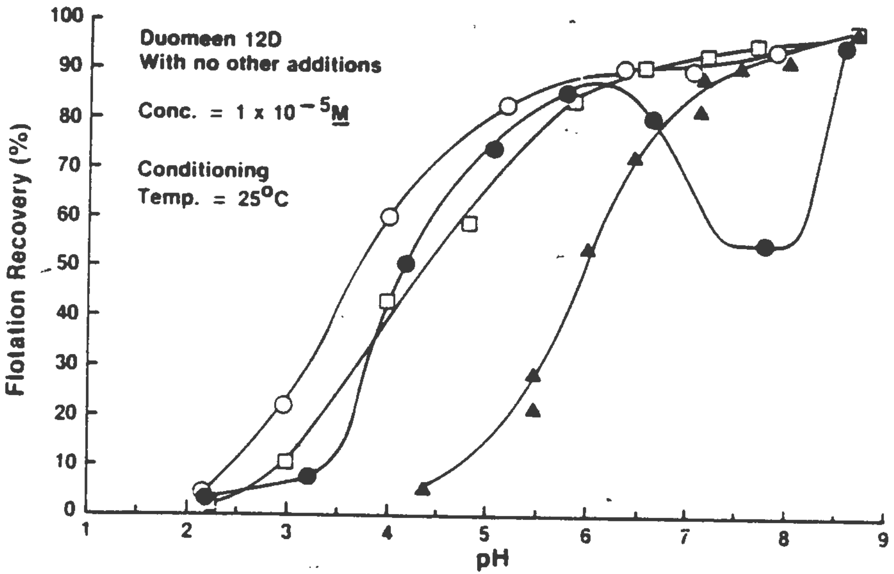

Figure 10a. The effect of quartz pretreatment on flotation recovery as a function of pH.

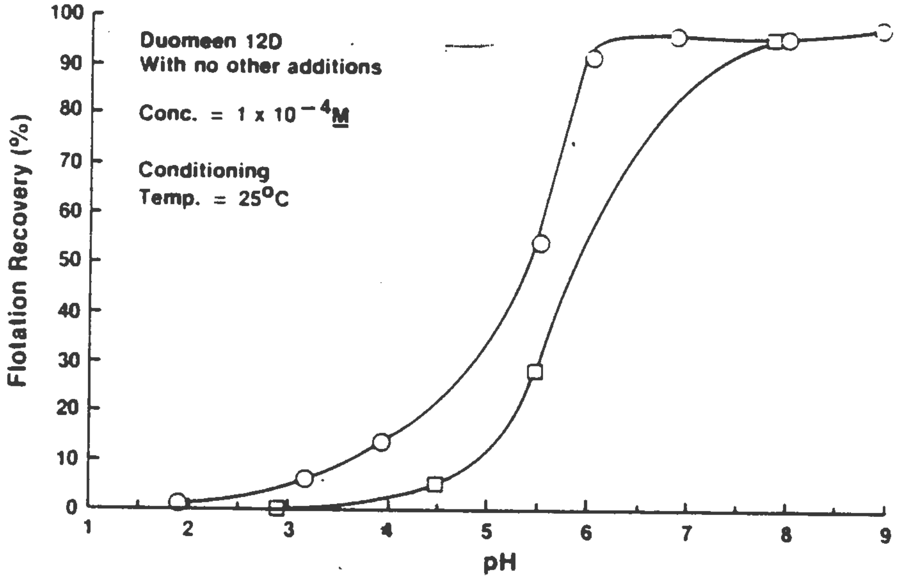

Figure 10b. The effect of quartz pretreatment on flotation recovery as a function of pH.

The Effects of Pretreatment and 12D Concentration on the Flotation Recovery and Adsorption of 12D on Quartz in the Presence of Collector Solution Only

Figure 11a shows the effects of quartz pretreatment on the flotation recovery of quartz as a function of pH in the presence of collector solution only, at varying concentrations. Figure 11b shows the adsorption of 12D on quartz, and zeta potential of quartz in pure water (Smith, 1982) as a function of pH in the presence of collector solution only.

Sample pretreatment for the open circle 5×10^{-4} $\underline{M}$ 12D curves and the closed triangle 10^{-5} $\underline{M}$ curves was conducted as noted in the experimental section. As mentioned earlier, the samples used for the open square 10^{-5} $\underline{M}$ 12D in Figure 11a were obtained from another graduate student. The samples used for the closed circle 10^{-6} $\underline{M}$ 12D curve were prepared under the same conditions as noted for the open square 10^{-5} $\underline{M}$ curve seen in Figure 10a.

Quartz crystals were first leached in concentrated, boiling HCl for 15 minutes, rinsed, dried, crushed to -65 +150 mesh, wet screened and oven-dried. It should be noted that quartz sample size used in the picric acid adsorption experiments reported in Figure 11b and following were conducted with 1.0 gram quartz samples. Comparing Figures 11a and 11b, it can be seen that quartz flotation recovery under some pretreatment conditions follows adsorption curves noted in Figure 11b. As collector concentration is increased, quartz flotation recovery is increased, as well as 12D adsorption.

An interesting occurrence is the adsorption of 12D from approximately pH 4 to pH 6, where the reported zeta potential of quartz is relatively low. This adsorption peak is followed by a decrease in adsorption from about pH 6 to pH 8.5. This decrease in adsorption and flotation recovery is attributed, in part, to weak adsorption forces occurring in this pH range. This will be discussed in detail in the following section.

It is interesting to note that this behavior is highly dependent on quartz pretreatment and collector concentration. The difference in the size fractions used for the adsorption and flotation experiments may also contribute to this observed behavior. Because surface area is increased for particles in the finer size fractions, the kinetics involved in the quartz surface reactions may be slightly different.

With regard to quartz pretreatment, it appears that surface reactions taking place vary as a function of particle surface area size, and shift the reactions to the left or right as noted in Equations 1 and 2. Therefore, close sizing with known distributions may be desirable in order to determine the extent of these reactions, and presumably aid in experimental reproducibility. The occurrence of the adsorption peaks in the lower pH ranges, as mentioned earlier, also corresponds with experimental pKa values reported by Smith and McGill for the 12D amine compound.

As can be seen from Figure 11a, some of the observed flotation recovery peaks also lie in the vicinity of the experimental pKa values noted for this compound. Observe the slight dip occurring at pH 9.28 for the open square 10^{-5} $\underline{M}$ curve in Figure 11a. In some of the following figures, quartz and magnetite flotation recovery curves will be seen to exhibit this type of behavior. At approximately pH 9.3, a decrease in bubble production and an increase in bubble size occurs. The reason for this is not clear, but may be linked to changes in surface tension exhibited by collector species as a function of pH. From pH 2 to pH 9.3, bubble production ranges from a dense tight froth to a less dense froth with larger bubble size. After pH 9.3, a slight decrease in bubble size was observed.

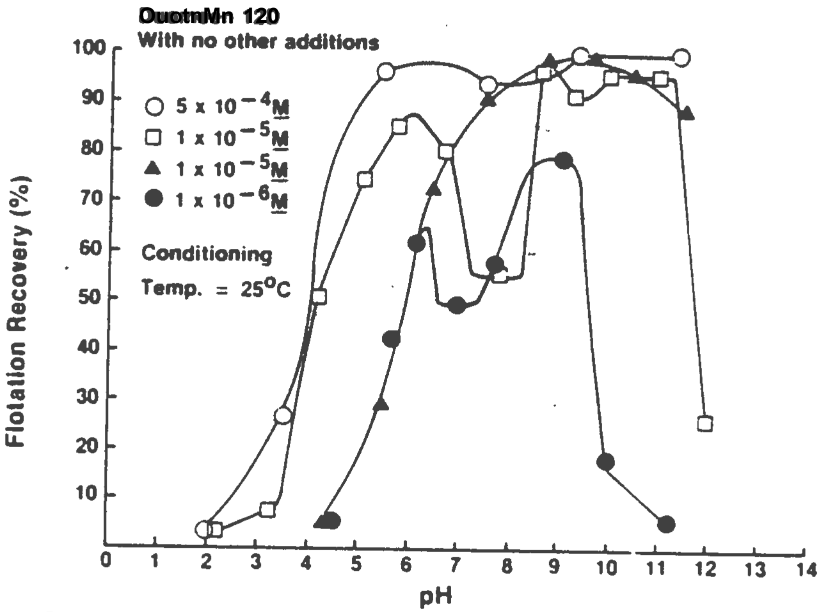

Figure 11a. Flotation recovery of quartz as a function of pH.

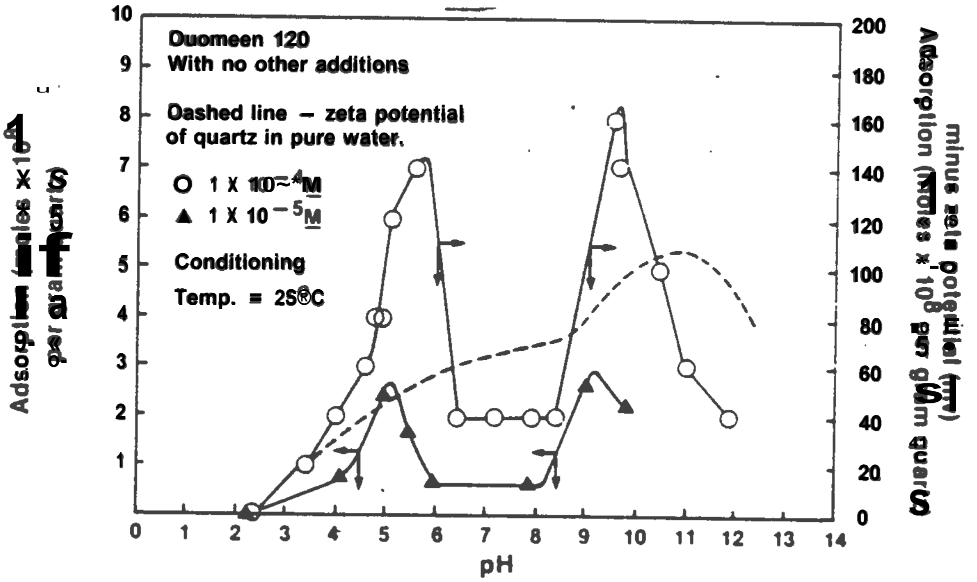

Figure 11b. Adsorption of Duomeen 12D on quartz as a function of pH

The Flotation Recovery of Quartz and Adsorption of 12D on Quartz as a Function of 12D Concentration in the Presence of Collector Solution Only, at pH 5.5, pH 7.5 and pH 9.5

Figures 12a and 12b show the effects of increasing 12D concentration on the flotation recovery and adsorption of 12D on quartz at pH 5.5, pH 7.5 and pH 9.5, in the presence of collector solution only. Because it was not possible to reproduce the results noted for the open square curve found in Figure 11a, the samples used for the closed circle 10^{-6} $\underline{M}$ 12D (11a) curve were also used for the results noted above in Figures 12a and 12b.

For the adsorption studies, the quartz flotation samples were lightly ground in a mortar and pestle, and then screened to -65 +325 mesh. This resulted in a shift in the size distribution towards the larger sizes and is reflected by the lower adsorption values. Only at 10^{-6} $\underline{M}$ at pH 7.5 is a decrease in flotation recovery seen. From about 5 x 10^{-5} $\underline{M}$ 12D to 10^{-3} $\underline{M}$ 12D, adsorption of 12D on quartz is seen to decrease at pH 7.5. In this region, 100 percent flotation recovery corresponds to an adsorption of about 5 x 10^{8} $\underline{M}$ 12D per gram quartz.

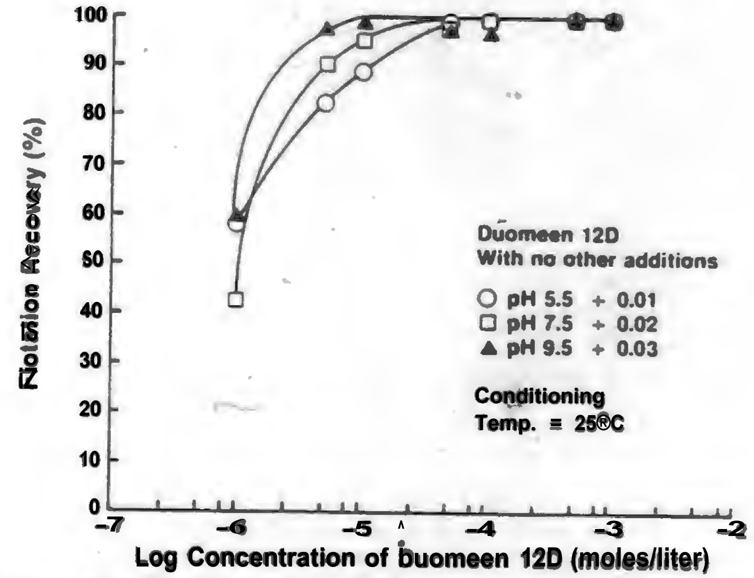

Figure 12a. Flotation recovery *of* quartz as a function of Duomeen 120 concentration.

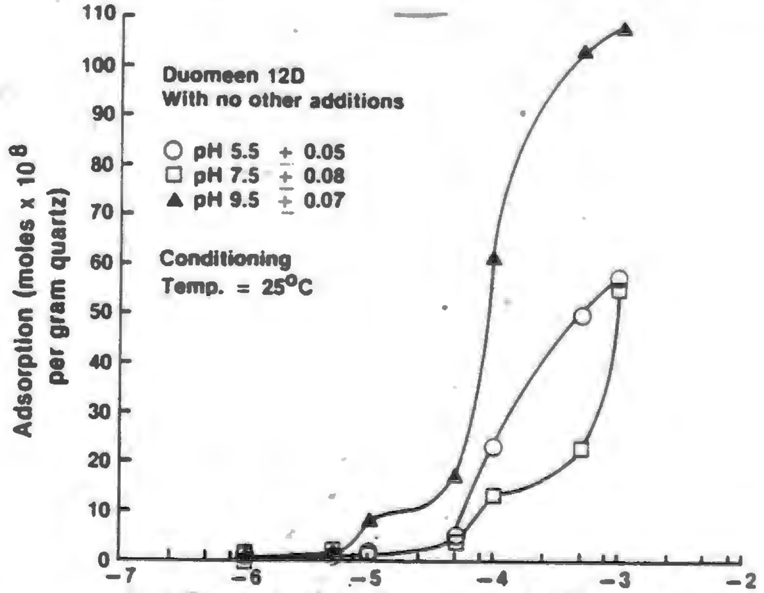

Figure 12b. Adsorption of Duomeen 120 on quartz as a function of unadsorbed 120 concentration.

The Effect of Pretreatment on the Flotation Recovery of Quartz Using 5 x 10^{-4} M, 10^{-4} M and 10^{-5} M 12A, in the Presence of Collector Solution Only

Figure 13 shows the effect of mineral pretreatment on the flotation recovery of quartz using Armeen 12D (Primary amine 12A), at varying concentrations as a function of pH, in the presence of collector solution only. The above flotation recovery curves correspond to the same collector concentration curves noted in Figures 10a and 11a, only the collectors are different.

The samples used for the open square 5 x 10^{-4} M 12A and closed triangle 10^{-5} M 12A curves were prepared as noted in the experimental section. The closed triangle curve is reproduced in Figure 18a.

The samples used for the closed circle 10^{-4} M 12A curve were prepared by first crushing quartz crystals to -65 +150 mesh, leaching in concentrated boiling HCl for 15 minutes, rinsing, wet screening and oven-drying at 95°C. This curve corresponds to the open square 10^{-4} M 12D curve found in Figure 10b, with regard to sample pretreatment.

The samples used for the open circle 10^{-5} M 12A curve were prepared as follows. Quartz crystals were first crushed to -65 +150 mesh, stored in double-distilled water for 24 hours, wet screened, and finally oven-dried at 95°C. This curve corresponds to the open square 10^{-5} M 12D curve noted in Figure 10a, with regard to sample pretreatment.

Comparing the above-mentioned curves, it can be seen that the diamine compounds exhibit slightly better flotation recovery in the lower pH range, with the exception of the 10^{-4} $\underline{M}$ 12A flotation recovery curve. As can also be seen, in Figure 13, the effect of quartz pretreatment has a similar affect for the 12A system, as compared with the 12D system. Flotation recovery is observed to be shifted in the alkaline direction, with respect to pretreatment.

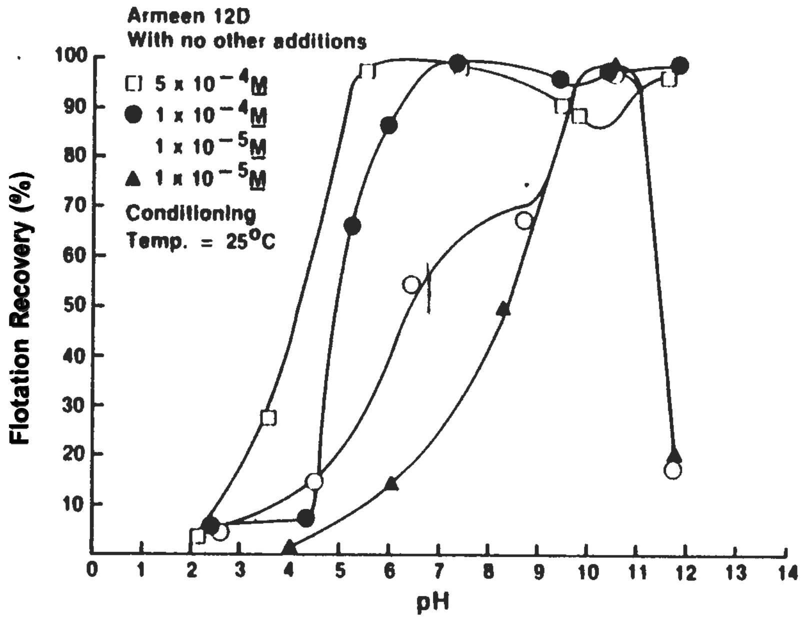

Figure 13. The effects of pretreatment and pH on the flotation recovery of quartz.

The Effect of Duomeen 16 Compound Purity on the Flotation Recovery of Quartz, with 0.1 M $CaCl_2$

Figure 14 shows the effects of 10^{-4} M Duomeen 16 compound purity and pH on the flotation recovery of quartz in the presence of 0.1 M $CaCl_2$ at 35°C. It should be noted that all 10^{-4} M Duomeen 16 flotation recovery experiments were conducted at 35°C. This was necessary because at 25°C, collector solutions containing the various salts were slightly cloudy. This measure aided in collector solubility. As can be seen in Figure 14, the less pure 16-carbon diamine compound gives slightly better quartz flotation recovery. This is because the less pure compound has a greater degree of varying hydrocarbon chain lengths present, which aid in selective adsorption in differing pH regions because of varying collector-solution properties.

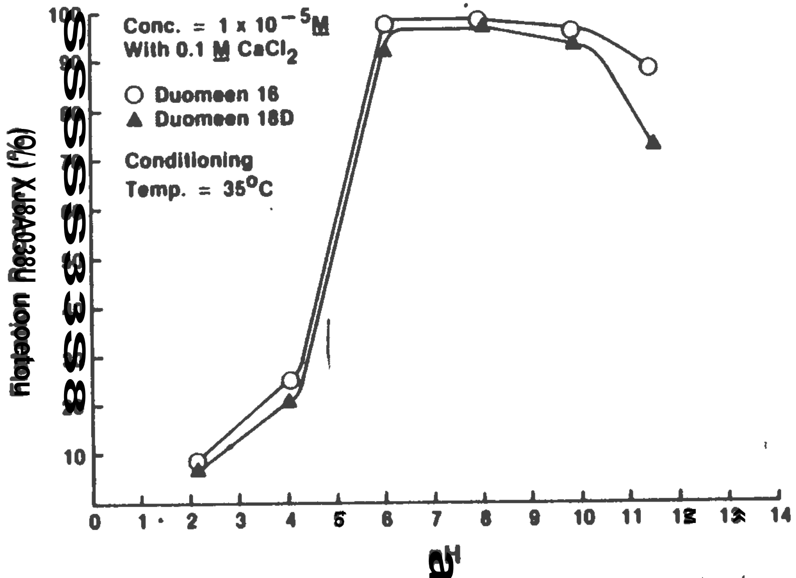

Figure 14. Flotation recovery of quartz as a function of pH.

The Effects of Temperature, pH, 10^{-5} $\underline{M}$ and 10^{-4} $\underline{M}$ 8D, 12D, 12A, and Duomeen 16 on the Flotation Recovery of Quartz and Magnetite, in the Presence of Collector Solution Only, with 0.6 $\underline{M}$ NaCl, with 0.1 $\underline{M}$ $CaCl_2$ and 0.1 $\underline{M}$ Na_2SO_4

Figures 15a through 25b show the flotation recovery of quartz and magnetite as a function of pH, using 10^{-5} $\underline{M}$, and 10^{-4} $\underline{M}$ 8D, 12D, 12A and Duomeen 16, in the presence of collector solution only, with 0.6 $\underline{M}$ NaCl, with 0.1 $\underline{M}$ $CaCl_2$, and with 0.1 $\underline{M}$ Na_2SO_4.

Included in the figures mentioned above is a study focusing on the effect of increasing conditioning temperature to 75°C for the 12D and 12A amine compounds. Adsorption of 10^{-5} $\underline{M}$ 12D on quartz and magnetite are also included in Figures 16b and 17b.

Most of the results reported in the following pages were from experiments conducted prior to learning about the importance of oxide-mineral pretreatment, so something should be said about the various batch sample preparations of quartz in order to correlate the data more effectively.

All magnetite experimental samples reported in the above-mentioned figures were prepared in a single batch. Experimental quartz sample batch (1) gave the following results, seen in Figures 15a (all curves), 18a (all curves), 20a (all curves), 22a (all curves), 23a (all curves) and 24a (all curves). Sample batch (2) gave the following results, seen in Figures 16a (all curves except open circle), 16b (all curves), and 21a (open circle curve only). Sample batch (3) gave the following results, seen in Figures 19a (all curves), 21a (all curves except open circle), and 25a (all curves). As will be seen in the above-mentioned figures, the effect of ionic strength at low collector concentrations results in a decrease in flotation recovery and adsorption. However, once the full adsorption potential of the various amines is reached, ionic strength has relatively little influence on flotation recovery. It will also be shown that quartz responds better to the various amine compounds than magnetite, for the experimental parameters investigated.

Figures 26a through 33b are a compilation of the curves found in Figures 15a, 15b, 16a, 17a, 18a, 18b, 19a, 19b, 20a, 20b, 21a, 21b, 23a, 23b, 25a and 25b. These figures show the relationship between collectors under the same experimental conditions.

Figures 15a and 15b show the relationship between quartz and magnetite flotation recovery using 10^{-5} $\underline{M}$ 8D under the same experimental conditions, as a function of pH. As can be seen, a reasonable separation of quartz from magnetite should be possible at approximately pH 9.5. However, the addition of the various salts results in a decrease in flotation recovery to about zero percent throughout the entire pH range. Under these conditions, the addition of the various salts is seen to function as a depressant in the quartz-magnetite flotation systems.

Figures 16a and 16b show the flotation recovery and adsorption of 10^{-5} $\underline{M}$ 12D on quartz, under the same experimental conditions, as a function of pH. Comparing Figures 16a and 16b, it can be seen that quartz flotation recovery correlates to adsorption studies for the collector-salt solutions. It is interesting to note that upon the addition of the various salts, the adsorption peak from pH 4.5 to 5.5 disappears. This is believed to be the result of ion competition within the double layer. It can also be seen that the addition of 0.1 M $CaCl_2$ has a greater depressing effect upon quartz flotation recovery than does the addition of the other two salts. This is attributed to a greater repulsion exhibited by the quartz surface, and thus, less 12D adsorption.

After about pH 7, adsorption for the various 12D solutions on quartz is seen to be approximately equal. Given the quartz flotation recovery curves noted in Figures 16a, this type of behavior should not be so. It is therefore felt that the collector-salt adsorption curves are in error, due to salt complexes that may have been formed in the picric acid-chloroform adsorption procedure, which caused a slight increase in the noted adsorption curves. With no salt additions, 100 percent quartz flotation recovery is seen to correspond to a 12D adsorption of about 3×10^{8} M per gram quartz at pH 9.7.

Figures 17a and 17b show the same conditions as noted above for quartz, except that magnetite is used. Comparing Figures 17a and 17b, it can be seen that magnetite flotation recovery corresponds extremely well with adsorption studies, with a 40 percent flotation recovery, corresponding to a

12D adsorption of 2.1×10^8 $\underline{M}$ per gram magnetite at pH 9.5.

Comparing Figures 16a, 16b, 17a and 17b, it can be seen that magnetite responds poorly, as compared with quartz, for the same experimental conditions, however, a suitable quartz-magnetite separation would not be possible.

Because the picric acid adsorption procedure was seen to be influenced to some extent by the addition of the various salts, the remaining figures deal exclusively with quartz and magnetite flotation recovery.

Figures 18a and 18b show the same experimental conditions for quartz and magnetite, except that 10^{-5} $\underline{M}$ Armeen 12D (12A) was used.

As can be seen in Figure 18a, quartz flotation recovery is least influenced by the addition of 0.1 $\underline{M}$ Na_2SO_4, with 0.1 $\underline{M}$ $CaCl_2$ having the greatest depressing effect. It is also interesting to note that upon the addition of the various salts, each quartz flotation recovery curve is shifted slightly to the left. This is due to a decrease in collector solubility. As can be seen in Figure 18b, magnetite flotation recovery is nonexistent, upon the addition of the various salts. Comparing the two figures, it can be seen that 10^{-5} $\underline{M}$ 12A functions as a better collector for quartz than for magnetite.

Comparing Figures 16a with 18a reveals that with no salt additions, the 12D compound gives much better quartz flotation recovery in the lower pH range, up to about pH 9. However, the 12A primary amine gives better flotation recovery from pH 10 to pH 11. This is due to the differences in the noted pKa values. All of the curves noted for the 12A compound are shifted slightly to the right of those noted for the 12D diamine compound. It is interesting to note that in the presence of 0.1 M Na_2SO_4, the 12A primary amine gives approximately 20 percent better flotation recovery for quartz than the 12D diamine, at pH 10. However, in the presence of 0.6 M NaCl and 0.1 M $CaCl_2$, the flotation recovery of quartz is seen to be better for the 12D diamine throughout the entire pH range. Also of interest, and evidenced in some of the following figures, is the slight increase in flotation recovery in the presence of 0.1 M $CaCl_2$ from pH 10 to pH 12. When the experiments were conducted, it was found that in this pH range, a precipitate was formed, which presumably increased collector solubility slightly.

Comparing Figures 17a and 18b, it can be seen that the 12D diamine gives approximately 10 percent better flotation recovery of magnetite from about pH 8 to pH 10 than the primary amine (Armeen 12D). Upon the addition of the various salts, magnetite flotation recovery is seen to drop off to about zero percent in both cases.

Figures 10a and 10b show the same experimental conditions as noted earlier, except Duomeen 16 is used. Quartz flotation recovery is seen to respond quite well under all conditions, with the salt additions shifting the flotation recovery curves in the alkaline direction. Magnetite flotation recovery is at a maximum at about pH 9, whereupon, the addition of the various salts results in a considerable decrease in flotation recovery. Comparing the two curves, it can be seen that under some conditions, a good quartz-magnetite separation is possible.

Comparing Figures 15a, 15b, 16a, 17a, 18a, 18b, 19a and 19b, the Duomeen 16 compound is revealed to function as a better collector for quartz from pH 2 to pH 12, under the noted experimental conditions. Whereas, magnetite flotation recovery is only slightly better in the presence of collector solution only, and drops off extensively upon the additions of the various salts, regardless of the collector, and increasing chain lengths. Upon the various salt additions, the addition of Na_2SO_4 least affects quartz flotation recovery for the 8D, 12D, and especially, the 12A amine compounds. The addition of NaCl decreases quartz flotation recovery the most for the 8D and 12A compounds, and least affects flotation recovery for the Duomeen 16 compound. In all cases, the addition of $CaCl_2$ influences quartz flotation recovery the most.

Figures 20a through 25b show the same conditions as noted above, except the various collector concentrations are increased 10 times. Figures 22a, 22b, 24a and 24b show the same conditions, except conditioning temperature was increased to 75°C. Figures 25a and 25b also show the same conditions, except conditioning temperature was 35°C for the 10^{-4} $\underline{M}$ Duomeen 16 flotation studies, which aided in prevention of collector precipitation. Comparing Figures 20a and 20b, flotation recovery is much better under all conditions for quartz. The addition of Na_2SO_4 is seen to have the least depressing effect, whereas, the addition of $CaCl_2$ has the most. Comparing Figures 21a and 21b shows that the addition of Na_2SO_4 acts as an activator for both minerals. It is interesting to note that for the case of quartz, $CaCl_2$ is also seen to function as an activator. Recall that the open circle 10^{-4} M 12D curve seen in Figure 21a is the result of quartz samples prepared in different batches and therefore, may not represent the true conditions exhibited in this system. As can be seen for magnetite flotation recovery, the addition of $CaCl_2$ has the most depressing effect on flotation recovery, excepting the sharp increase in flotation recovery from pH 9 to pH 11.5.

With the exception of the $CaCl_2$ curve noted for magnetite, after pH 7, flotation recovery for both minerals is extremely good and is seen to be much better than the corresponding 8D collector.

Comparing Figures 22a with 21a and 22b with 21b, it can be seen that increasing conditioning temperature to 75°C results in a decrease in flotation recovery in the lower pH range. However, after approximately pH 7, quartz flotation recovery is seen to be slightly improved, except at pH 11.7, with the addition of $CaCl_2$. Magnetite flotation improves from pH 8 to pH 9, but falls off with the additions of the various salts. Regardless of conditioning temperature, the addition of Na_2SO_4 acts as a mild activator for both mineral systems in the lower pH range. Note the decrease in flotation recovery occurring at approximately pH 9.3.

With Figures 23a and 23b, a comparison of quartz and magnetite flotation recovery using 12A can be made. As can be seen, from pH 3 to pH 5.5, slightly better magnetite flotation recovery is possible in the presence of the various salts. However, in the presence of no salt additions, quartz flotation recovery is better.

Comparing Figures 23a and 21a, a reverse situation is noted for the 12A and 12D amines. The 10^{-4} M open circle flotation recovery curves for both figures in the lower pH range are essentially the same.

Comparing Figures 23b with 21b, the 12D compound is seen to function as a better collector for magnetite, under the noted conditions.

Comparing Figures 24a and 24b, it can be seen that flotation recovery for magnetite with the various salt solutions present is slightly better than for quartz in the lower pH range, with the various salt additions acting as mild activators from pH 3 to pH 6, in the 12A system.

Comparing Figures 24a with 23a indicates that quartz flotation recovery is decreased slightly for all curves in the lower pH range, with an increase in temperature.

Figures 24b and 23b indicate that an increase in conditioning temperature has little effect on magnetite flotation recovery in the Armeen 12D system.

Comparing Figures 24a and 22a, quartz flotation recovery is seen to be very close for both systems, with the exception of the points around pH 9.3. The same can be said of the magnetite flotation recovery curves seen in Figures 24b and 22b.

Figures 25a and 25b show the same conditions as noted earlier, but Duomeen 16 is used as the collector at 35°C.

The flotation characteristics for both minerals are approximately the same, with $CaCl_2$ having the least effect in the lower pH range, and Na_2SO_4 having the most pronounced effect. With no salt additions, the occurrence of two flotation peaks is noted for both minerals. These correspond closely to the Duomeen 16 pKa values. Upon salt addition, these flotation recovery peaks disappear. This type of behavior would suggest that upon addition of a salt, charge interaction of the two collector species is countered by the charge of the various ions in solution, in the electrical double layer.

Comparing Figures 20a, 20b, 21a, 21b, 22a, 22b, 23a, 23b, 24a, 24b, 25a and 25b, it can be seen that as collector chain length is increased, so is flotation recovery for both quartz and magnetite. Flotation recovery for both minerals varies extensively under the noted experimental conditions. Temperature has a slight depressing effect on quartz flotation recovery and relatively little effect on magnetite flotation recovery at 75°C.

As mentioned earlier, Figures 26a through 33b are a compilation of the 10^{-5} M and 10^{-4} M amine flotation studies conducted at 25°C and 35°C. These figures illustrate the differences between collectors under the same experimental conditions. For ease of comparison, the 10^{-5} M curves are first presented, followed by the 10^{-4} M flotation recovery curves.

Figures 26a, 26b, 27a and 27b show the effects of the various collectors on the flotation recovery of quartz and magnetite at 10^{-5} $\underline{M}$ and 10^{-4} $\underline{M}$ concentrations, in the presence of collector solution only.

Comparing Figures 26a with 26b, it can be seen that a good quartz-magnetite separation is possible, especially in the lower pH range with Duomeen 16. It is noteworthy that differences in collector chain length correspond to different regions of maximum flotation recovery for the two minerals. At the higher pH values, the longer-chained compounds are seen to shift maximum flotation recovery peaks in the acidic direction. This is due to differences in collector solution properties, and is reflected in the flotation recovery of the respective oxide minerals. Comparing Figures 27a and 27b, the shift in the acidic direction is not as apparent.

Comparing Figures 27a with 26a and 27b with 26b, it can be seen that as collector chain length and collector concentration are increased, flotation recovery is increased. In most cases, quartz and magnetite flotation recovery is seen to be better using the 12D compound than it is with the 12A compound.

Figures 28a, 28b, 29a and 29b show the effects of the various collectors on the flotation recovery of quartz and magnetite at 10^{-5} $\underline{M}$ and 10^{-4} $\underline{M}$ concentrations, with 0.6 $\underline{M}$ NaCl. Comparing the above figures, it can be seen that at the lower concentration, the Duomeen 16 compound gives better flotation recovery and that flotation recovery using 12D is better than that using the 12A amine compound. This same relationship is also observed for the flotation recovery magnetite at 10^{-5} $\underline{M}$ and 10^{-4} $\underline{M}$ concentrations, in the presence of collector solution only.

Comparing Figures 26a with 26b, it can be seen that a good quartz-magnetite separation is possible, especially in the lower pH range with Duomeen 16. It is noteworthy that differences in collector chain length correspond to different regions of maximum flotation recovery for the two minerals. At the higher pH values, the longer-chained compounds are seen to shift maximum flotation recovery peaks in the acidic direction. This is due to differences in collector solution properties, and is reflected in the flotation recovery of the respective oxide minerals. Comparing Figures 27a and 27b, the shift in the acidic direction is not as apparent.

Comparing Figures 27a with 26a and 27b with 26b, it can be seen that as collector chain length and collector concentration are increased, flotation recovery is increased. In most cases, quartz and magnetite flotation recovery is seen to be better using the 12D compound than it is with the 12A compound.

Figures 28a, 28b, 29a and 29b show the effects of the various collectors on the flotation recovery of quartz and magnetite at 10^{-5} $\underline{M}$ and 10^{-4} $\underline{M}$ concentrations, with 0.6 $\underline{M}$ NaCl. Comparing the above figures, it can be seen that at the lower concentration, the Duomeen 16 compound gives better flotation recovery and that flotation recovery using 12D is better than that using the 12A amine compound. This same relationship is also observed for the flotation recovery curves noted in Figures 29a and 29b, with the exception of quartz flotation recovery above pH 7.7, seen in Figure 29a.

Figures 30a, 30b, 31a and 31b show the effects of the various collectors on the flotation recovery of quartz and magnetite at 10^{-5} M and 10^{-4} M concentrations, with 0.1 M $CaCl_2$. Comparing these curves reveals that the 12D compound functions as a better collector for both quartz and magnetite than does the 12A compound. Also, quartz flotation recovery using 12D and Duomeen 16 diamines seen in Figure 31a is approximately the same from pH 2 to pH 5.

Figures 32a, 32b, 33a and 33b show the effects of the various collectors on the flotation recovery of quartz and magnetite at 10^{-5} M and 10^{-4} M concentrations, with 0.1 M Na_2SO_4. In Figure 32a, Armeen 12D is seen to give better quartz flotation recovery from pH 9.7 to pH 11.7 than Diamine 12D. Note the shift in the alkaline direction for the Armeen 12D curve. In Figures 33a and 33b, Na_2SO_4 is seen to act as an activator for the quartz and magnetite 12D systems from pH 2 to about pH 7.

Comparing Figures 26a through 33b, in most cases, the 12D diamine is seen to be a better collector for quartz and magnetite than the primary amine, Armeen 12D. The choice of any one collector, as has been shown, for the separation of quartz and magnetite, is dependent on the solution properties exhibited by the given collector. As collector chain length and concentration are increased, a notable increase in quartz and magnetite flotation recovery is seen. The pH of maximum flotation, however, is dependent upon the salts present and is seen to shift flotation recovery curves in these amine systems to the lower pH values in most cases, as compared with a system with no salt additions.

It should be mentioned that some of the flotation results observed agree with the work of Smith and Chini (Smith and Chini, 1980).

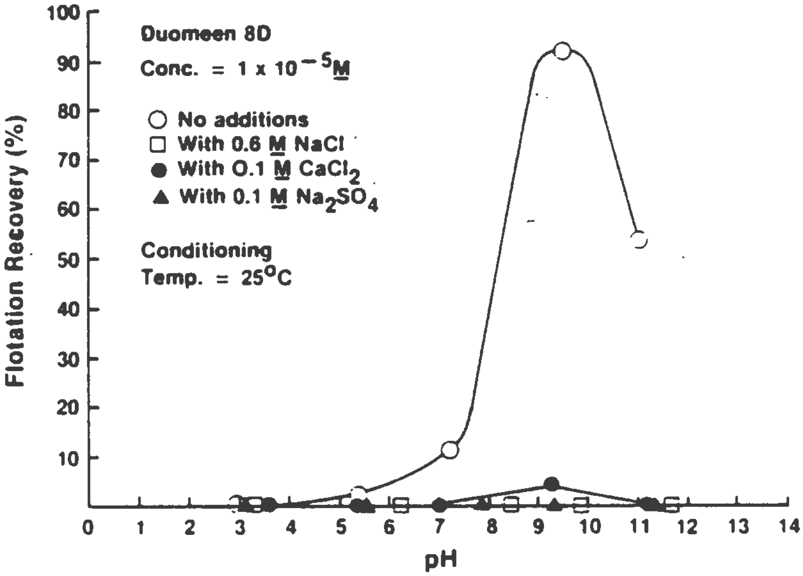

Figure 15a. Flotation recovery of quartz as a function of pH.

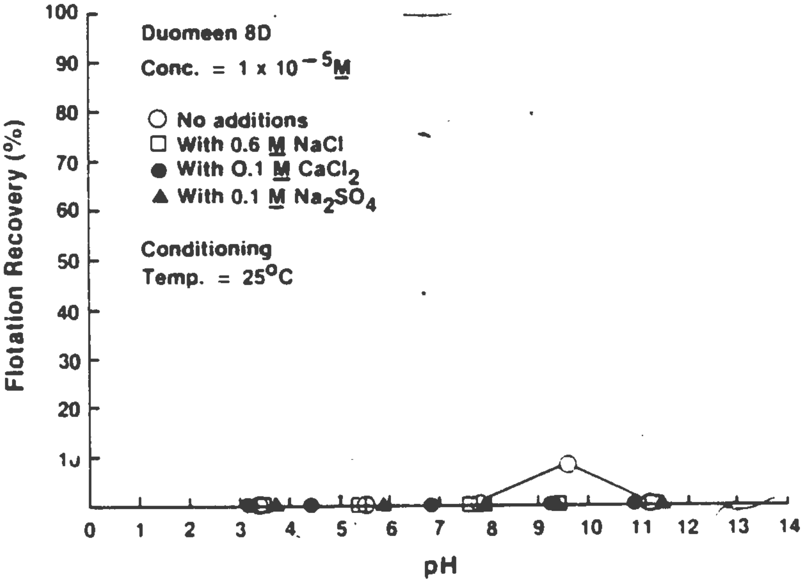

Figure 15b. Flotation recovery of magnetite as a function of pH.

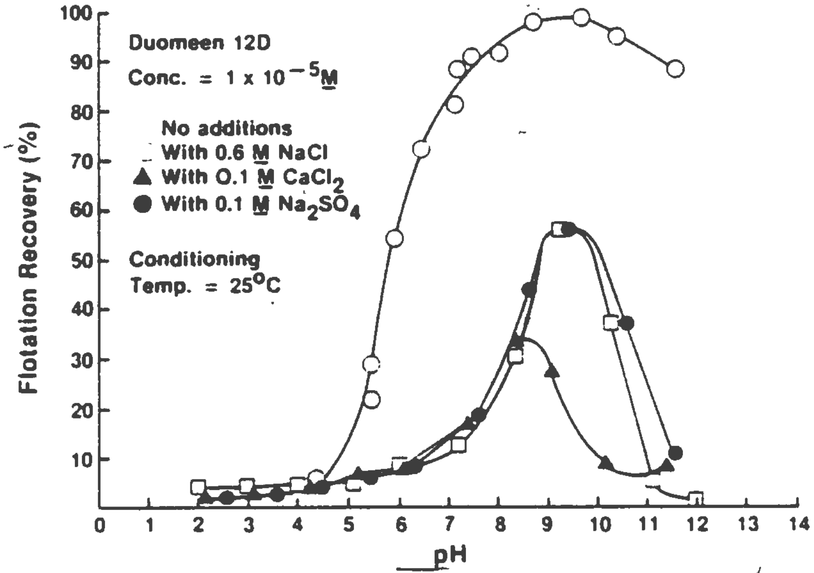

Figure 16a. Flotation recovery of quartz as a function of pH.

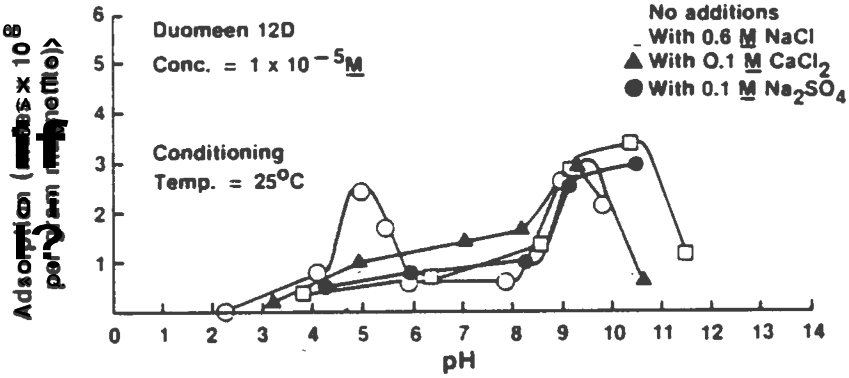

Figure 16b. Adsorption of Duomeen 12D on quartz as a function of pH.

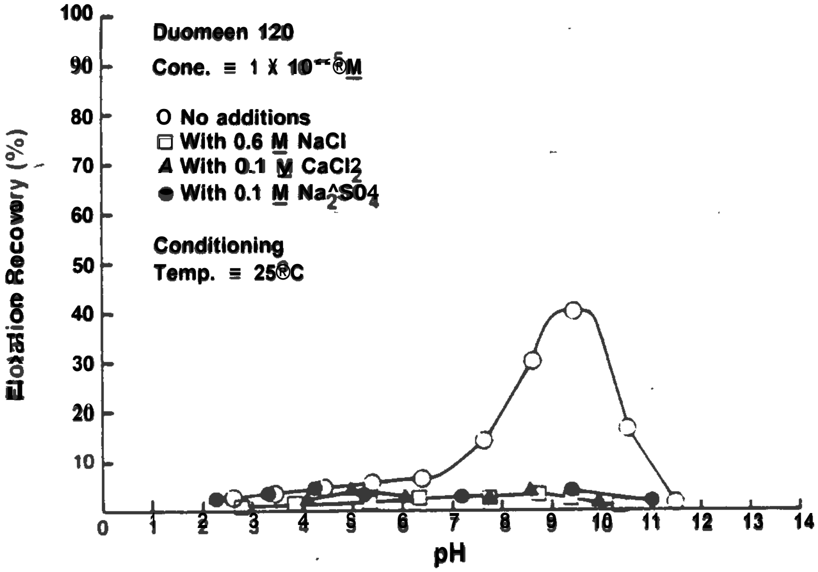

Figure 17a. Flotation recovery of magnetite as a function of pH.

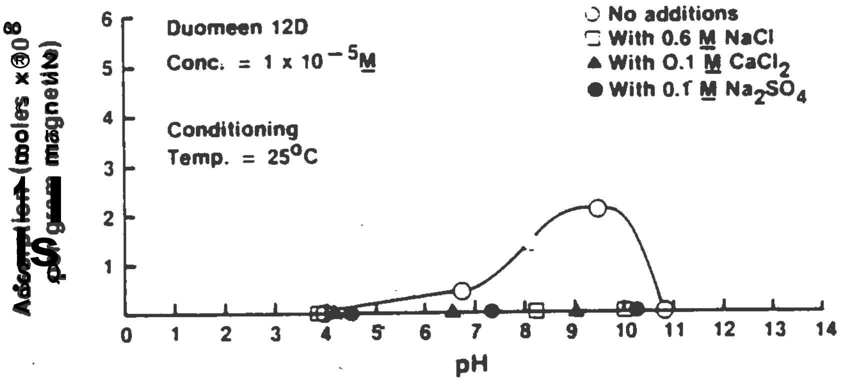

Figure 17b. Adsorption of Duomeen 12D on magnetite as a function of pH.

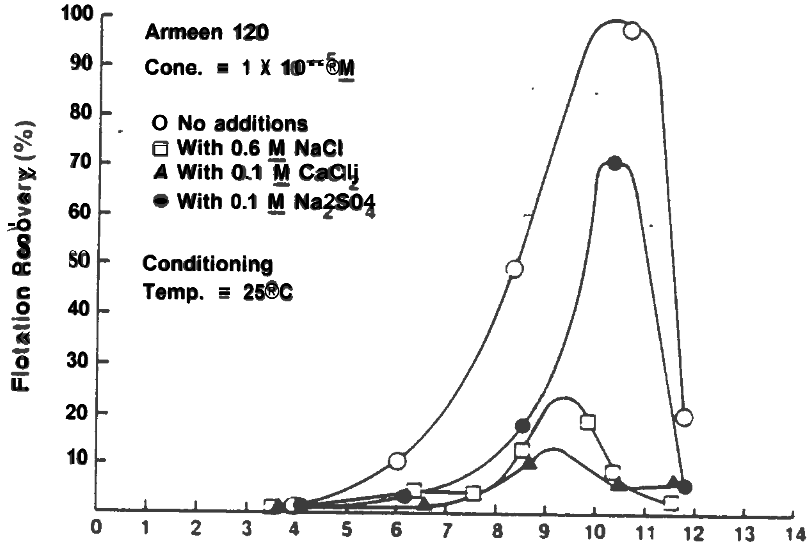

Figure 18a. Flotation recovery of quartz as a function of pH.

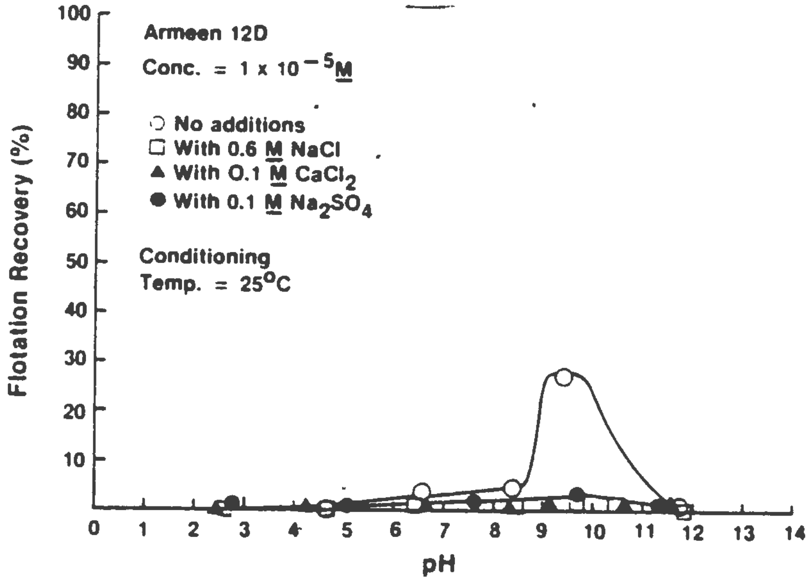

Figure 18b. Flotation recovery of magnetite as a function of pH.

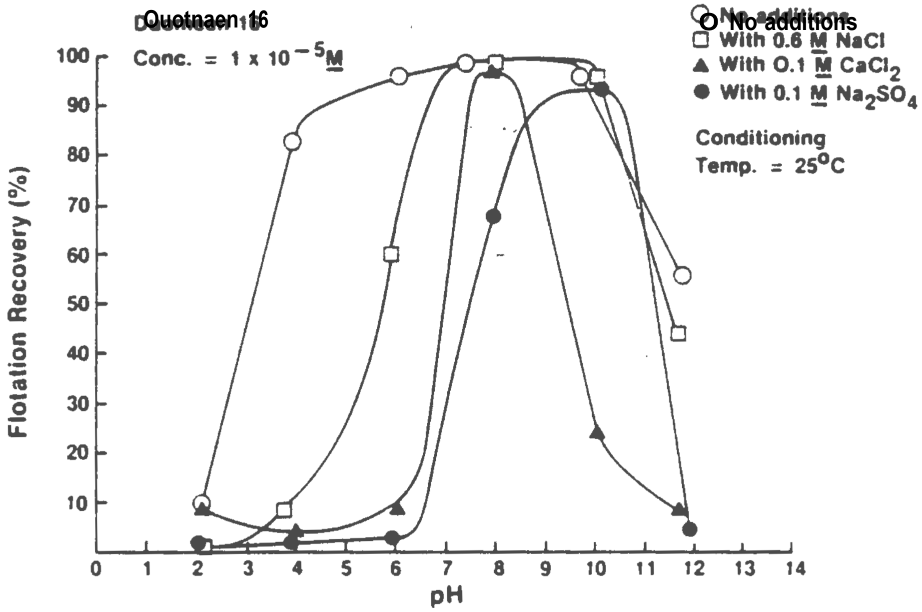

Figure 19a. Flotation recovery of quartz as a function of pH.

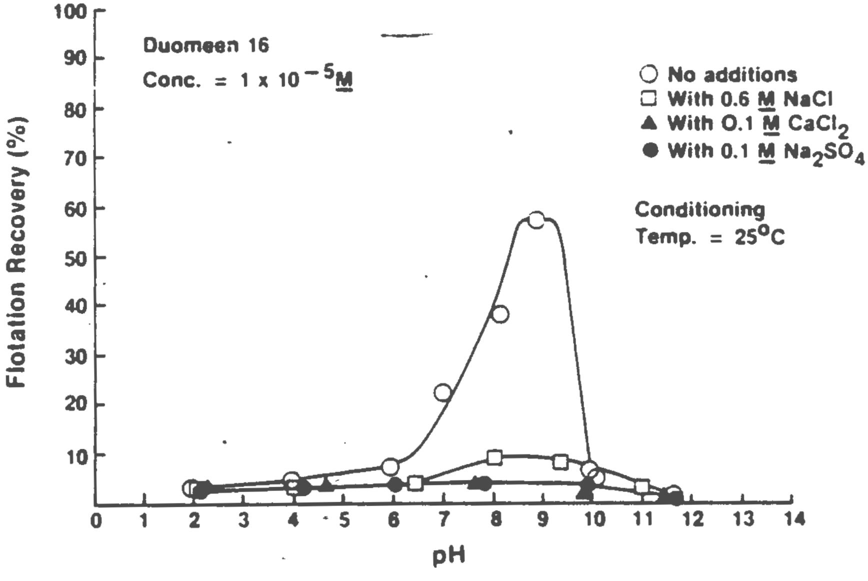

Figure 19b. Flotation recovery of magnetite as a function of pH.

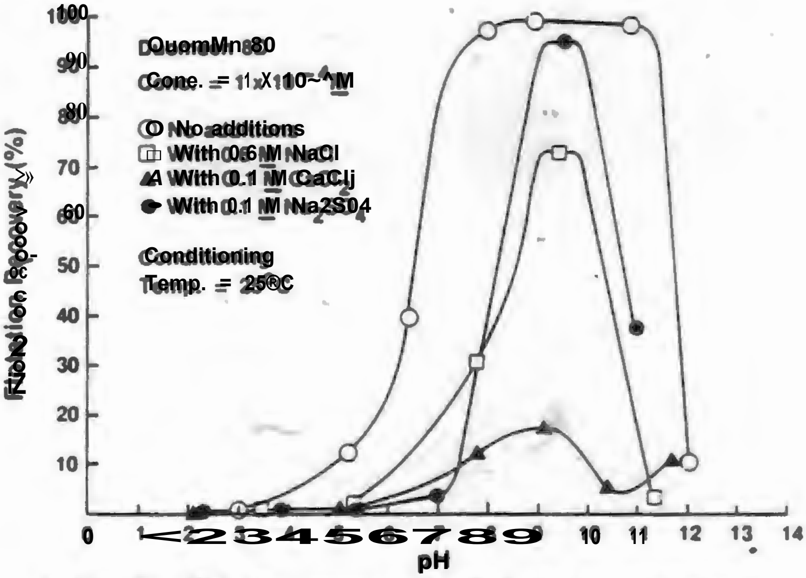

Figure 20a. Flotation recovery of quartz as a function of pH.

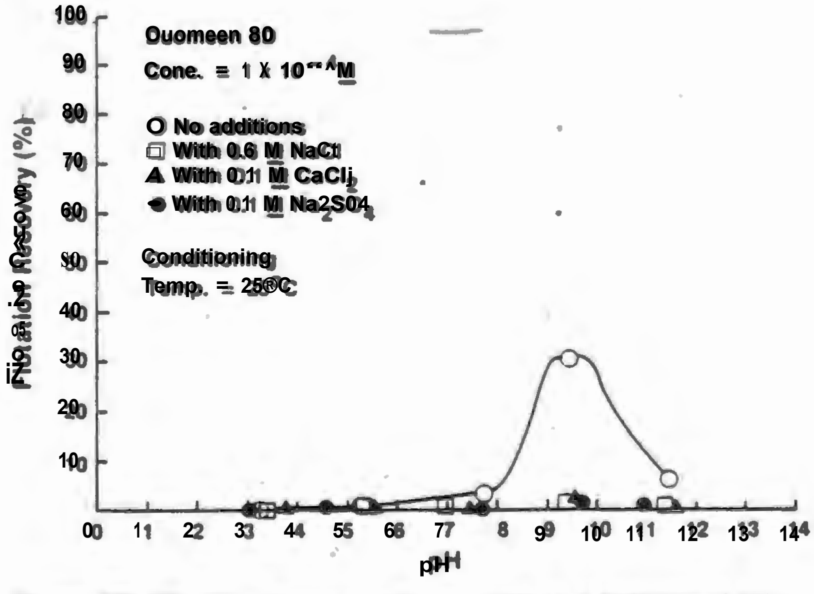

Figure 20b. Flotation recovery of magnetite as a function of pH.

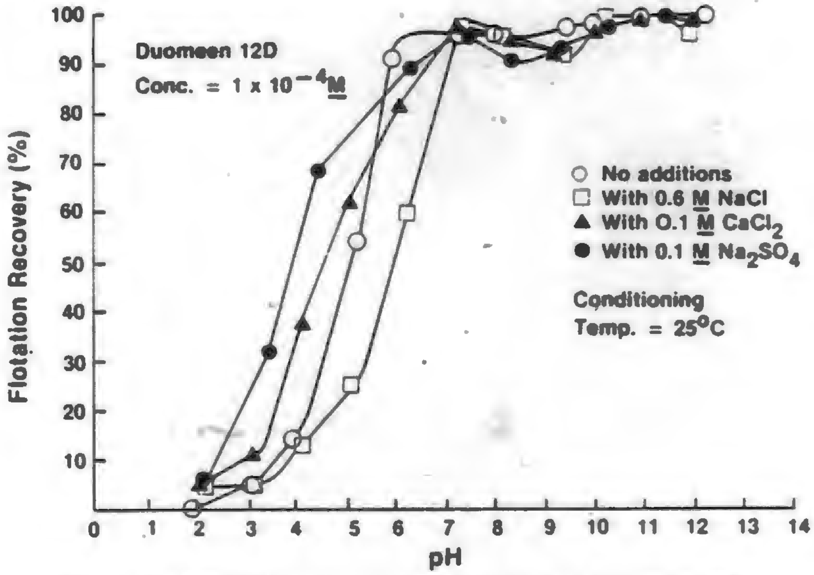

Figure 21a. Flotation recovery of quartz as a function of pH.

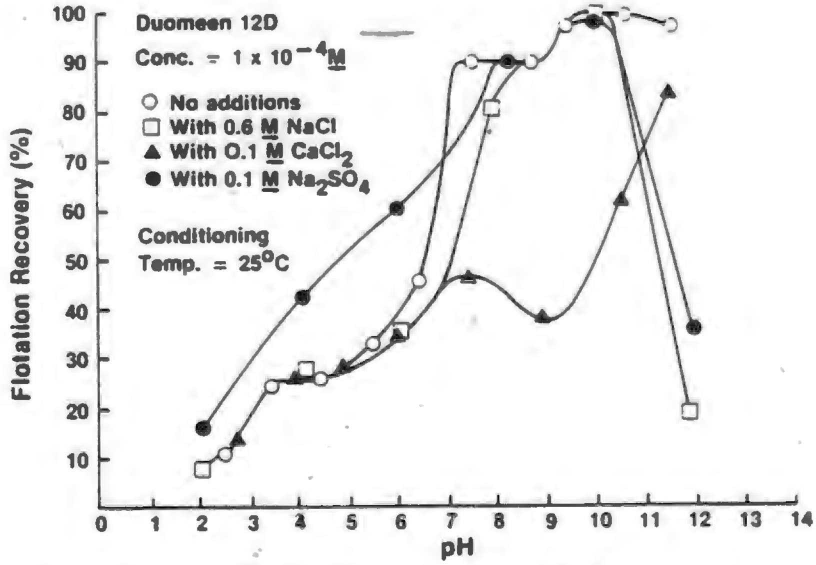

Figure 21b. Flotation recovery of magnetite as a function of pH.

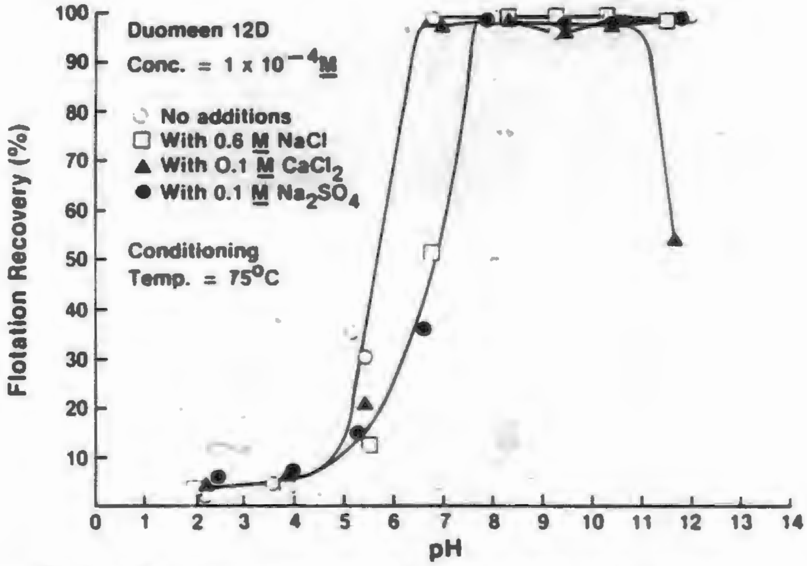

Figure 22a. Flotation recovery of quartz as a function of pH.

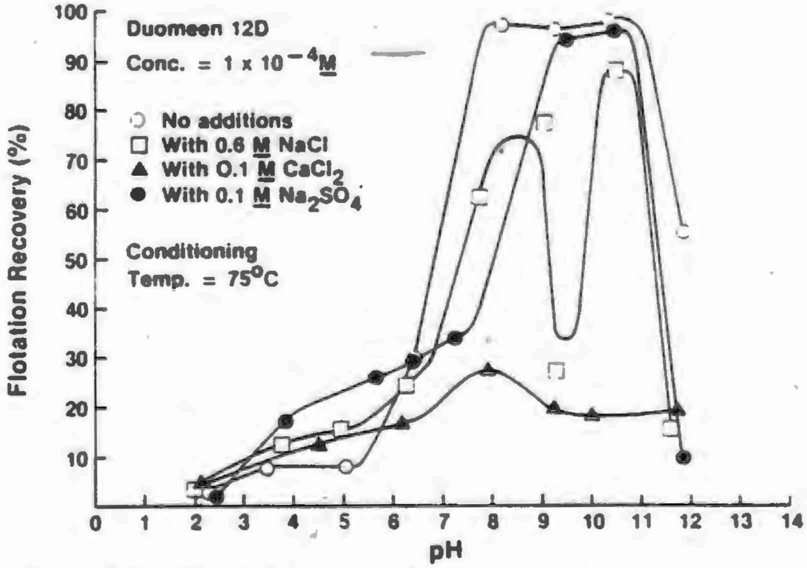

Figure 22b. Flotation recovery of magnetite as a function of pH.

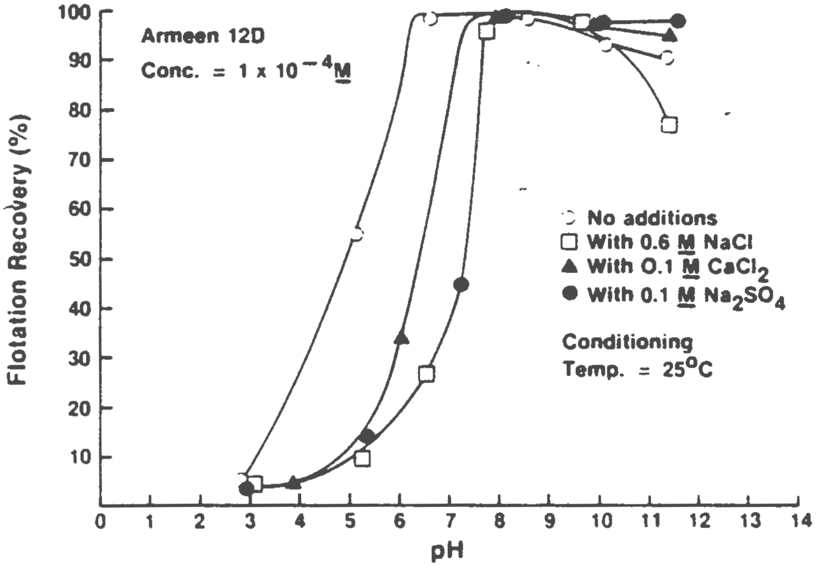

Figure 23a. Flotation recovery of quartz as a function of pH.

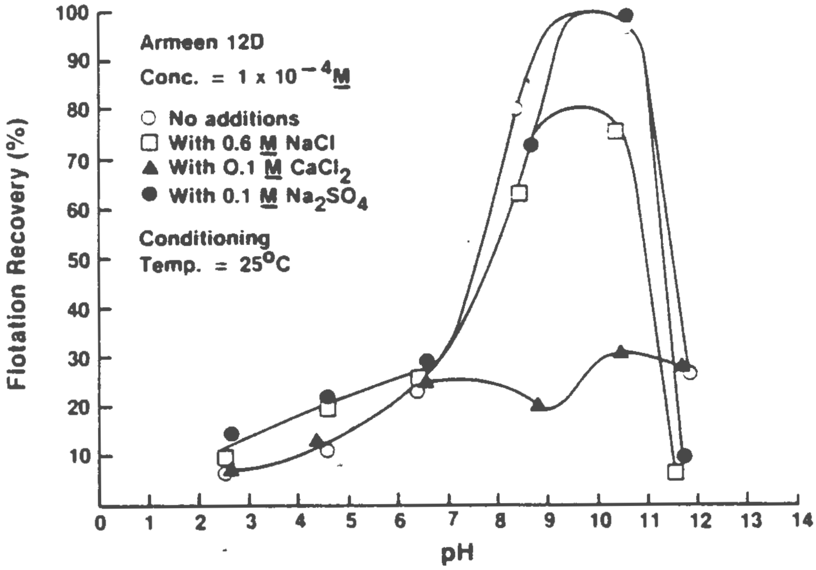

Figure 23b. Flotation recovery of magnetite as a function of pH.

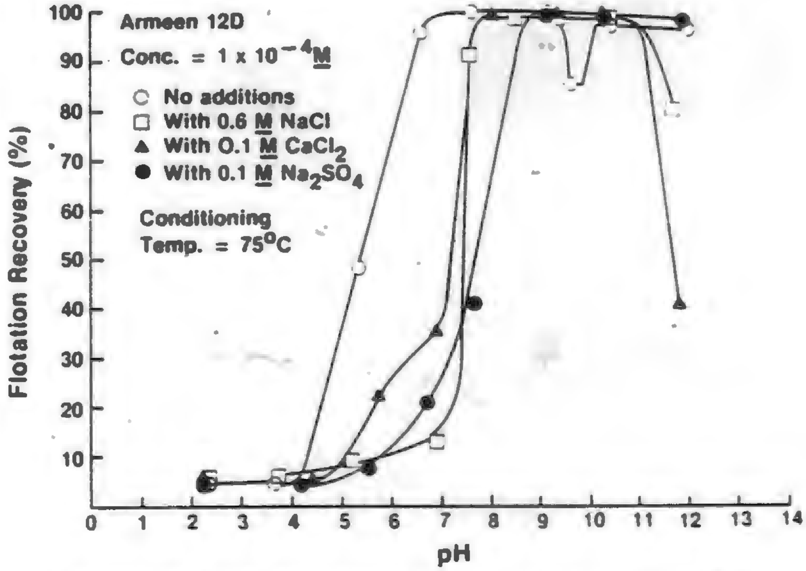

Figure 24a. Flotation recovery of quartz as a function of pH.

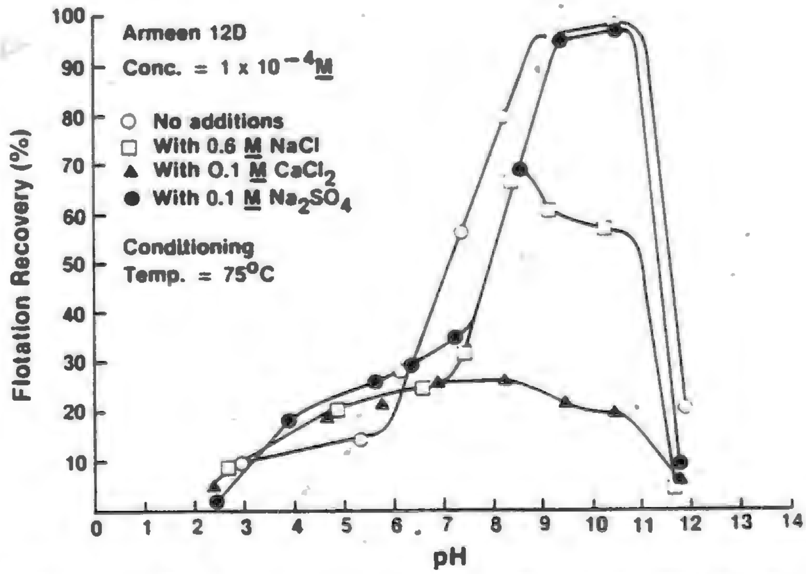

Figure 24b. Flotation recovery of magnetite as a function of pH.

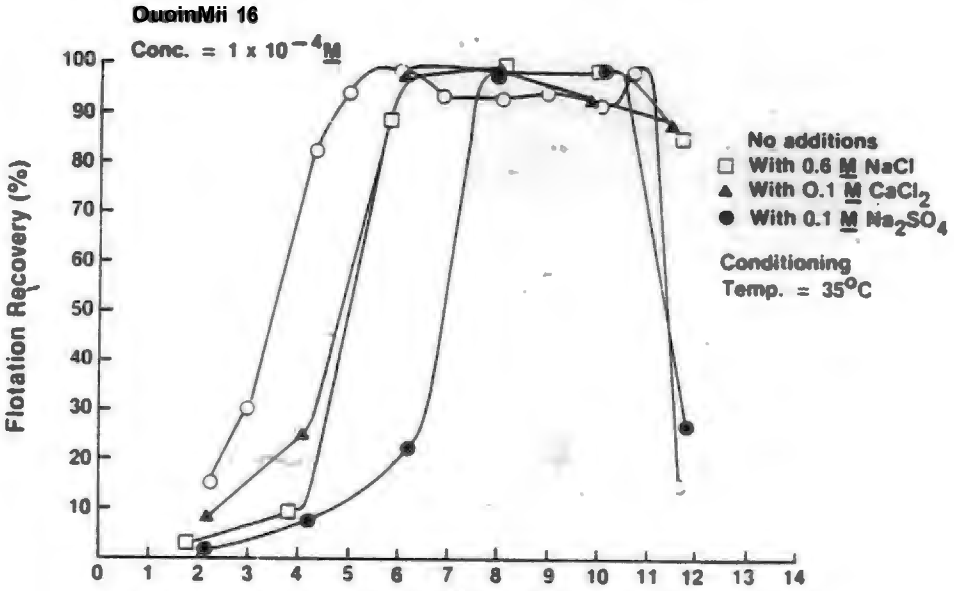

Figure 25a. Rotation recovery of quartz as a function of pH.

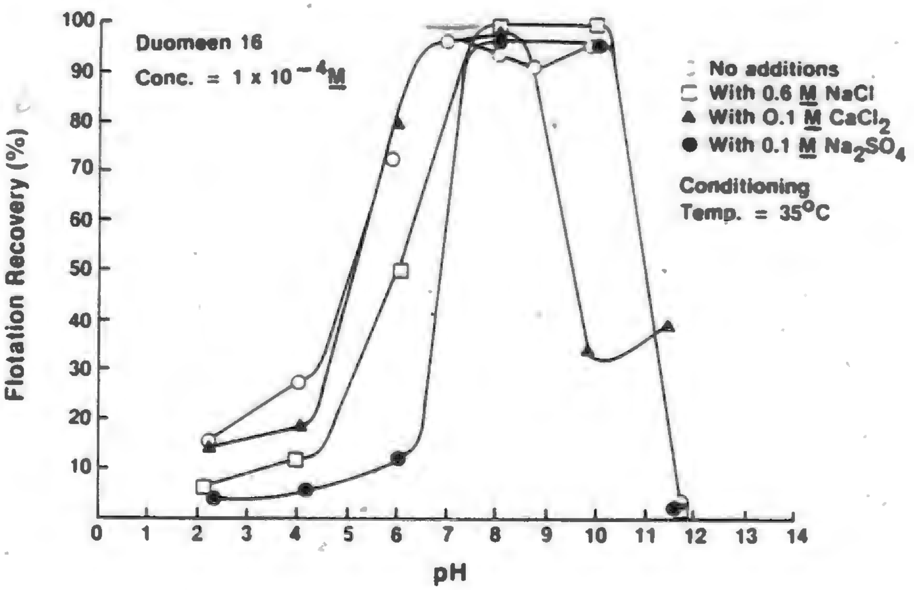

Figure 25b. Flotation recovery of magnetite as a function of pH.

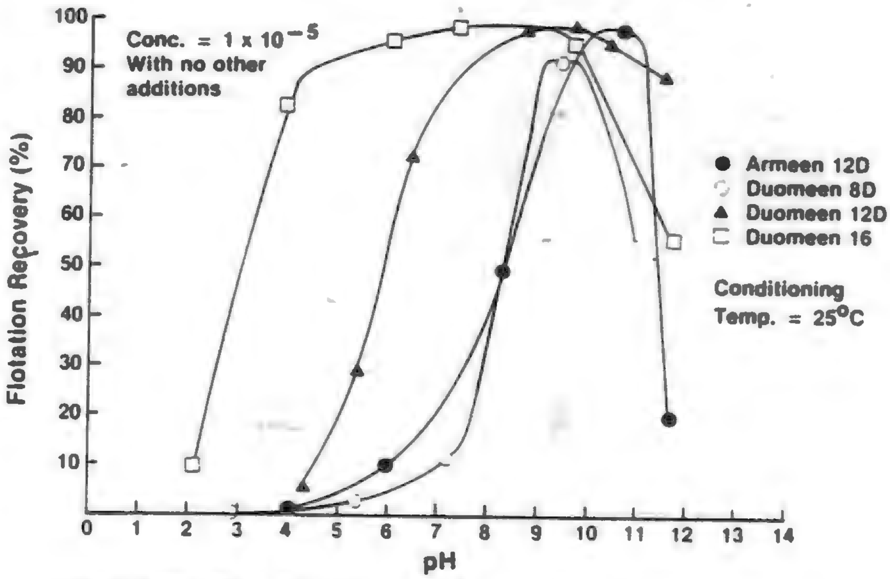

Figure 26a. Flotation recovery of quartz as a function of pH.

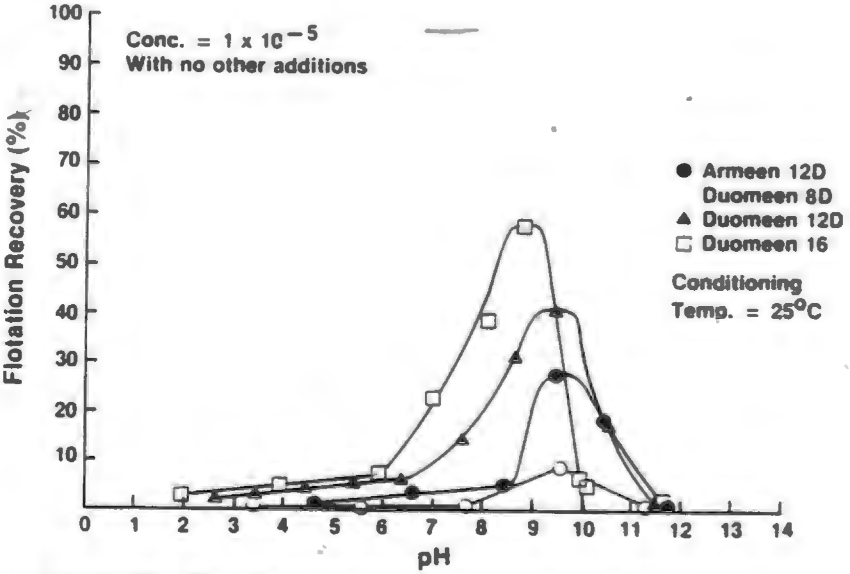

Figure 26b. Flotation recovery of magnetite as a function of pH.

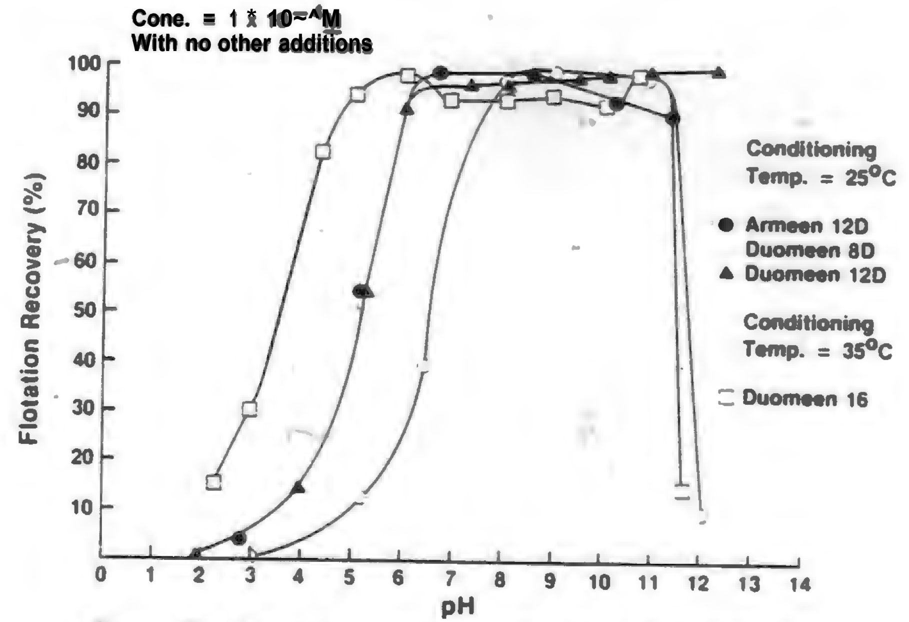

Figure 27a. Flotation recovery of quartz as a function of pH.

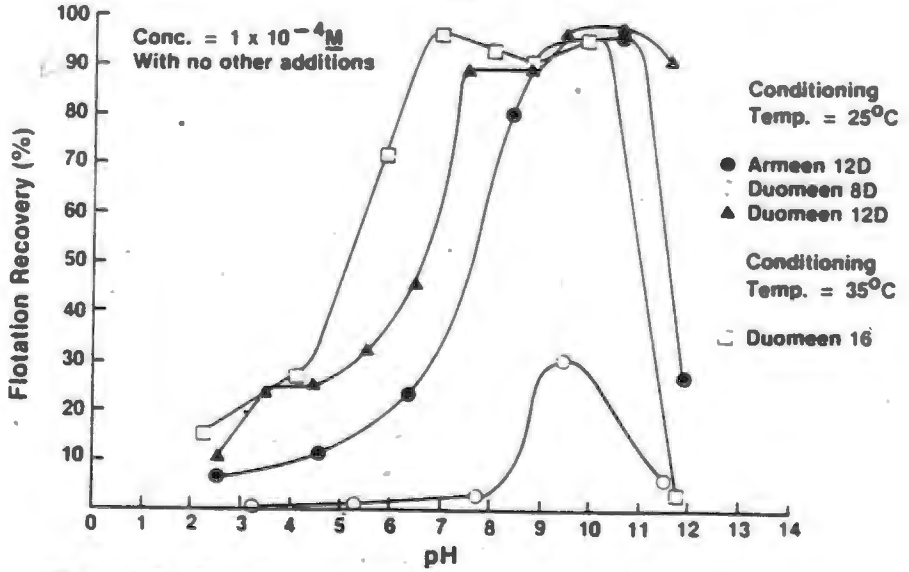

Figure 27b. Rotation recovery of magnetite as a function of pH.

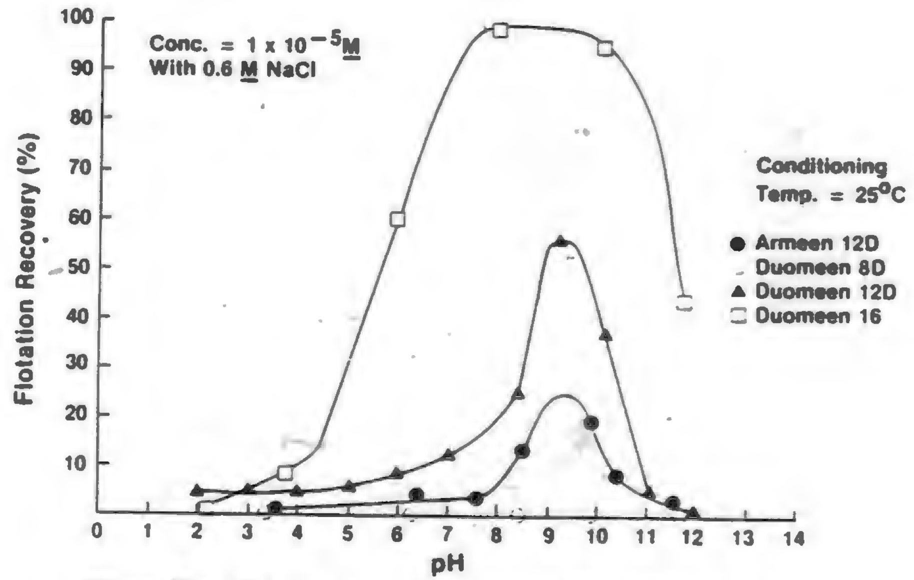

Figure 28a. Flotation recovery of quartz as a function of pH.

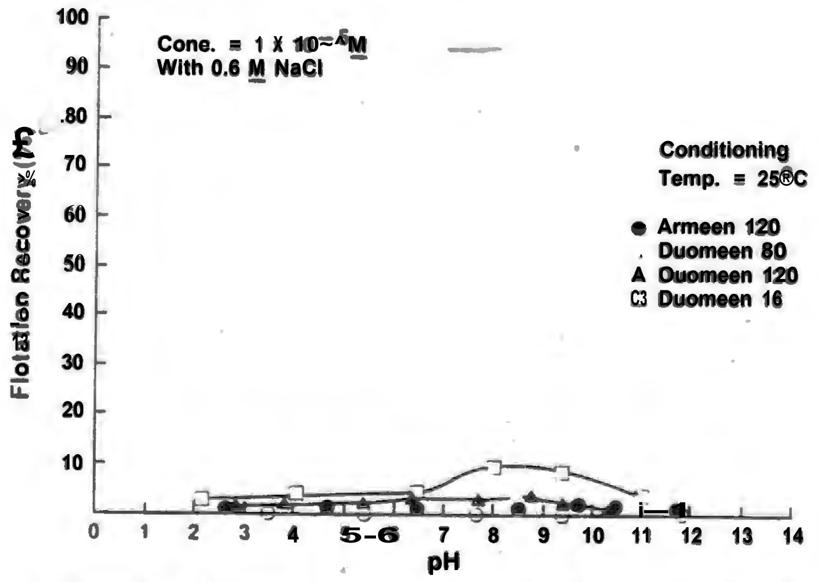

Figure 28b. Flotation recovery of magnetite as a function of pH.

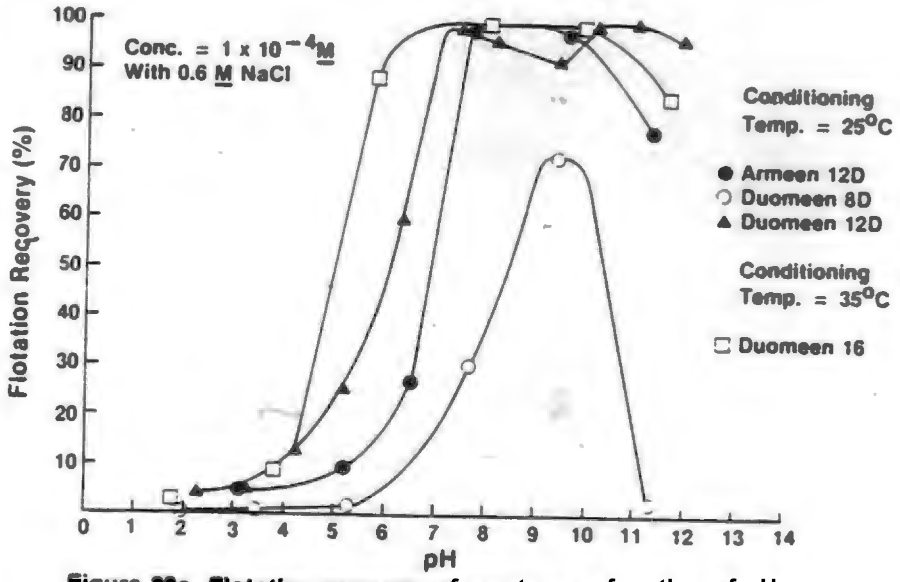

Figure 29a. Flotation recovery of quartz as a function of pH.

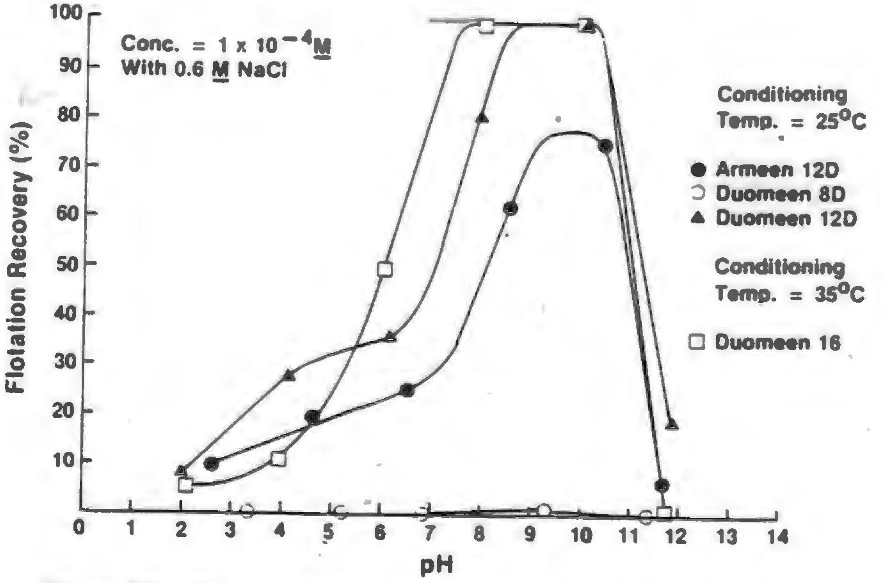

Figure 29b. Flotation recovery of magnetite as a function of pH.

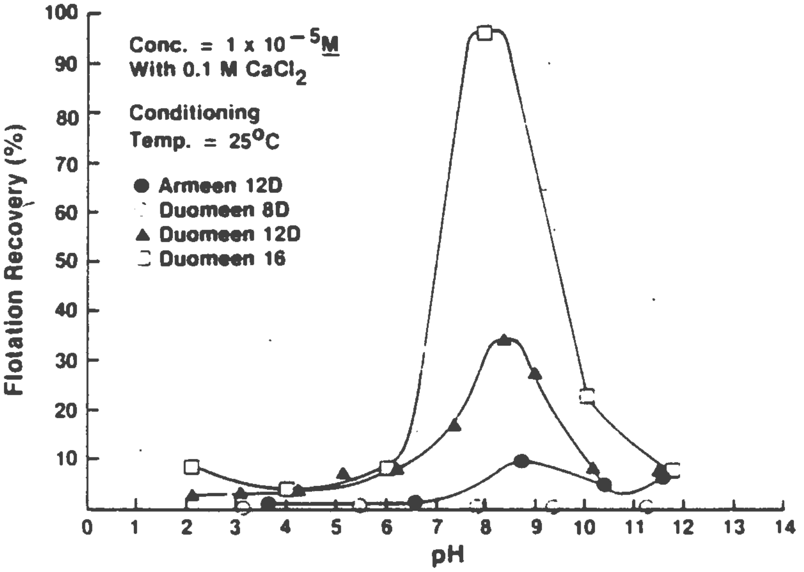

Figure 30a. Flotation recovery of quartz as a function of pH.

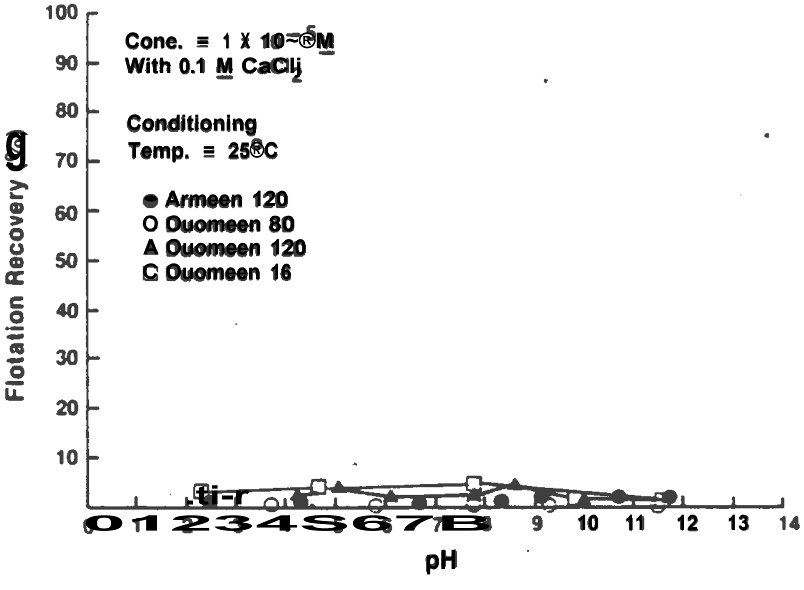

Figure 30b. Flotation recovery of magnetite as a function of pH.

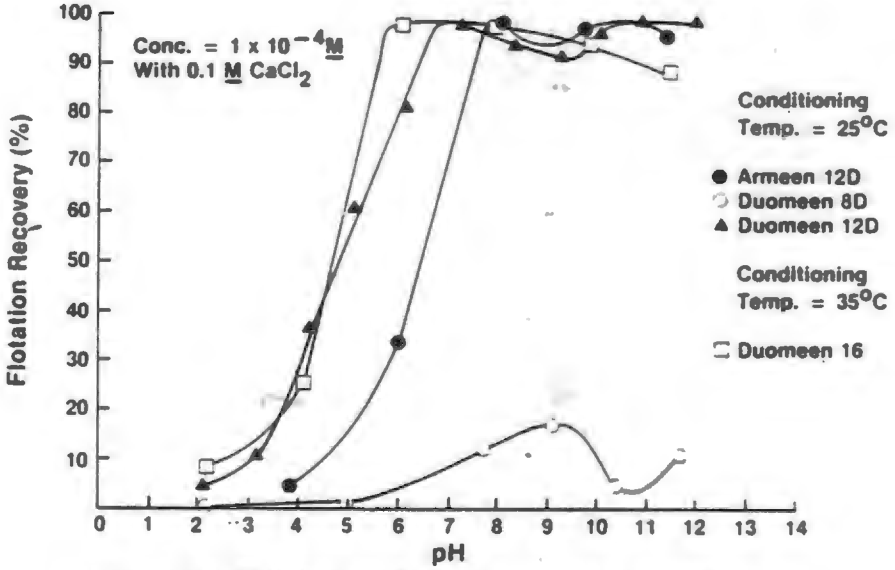

Figure 31a. Flotation recovery of quartz as a function of pH.

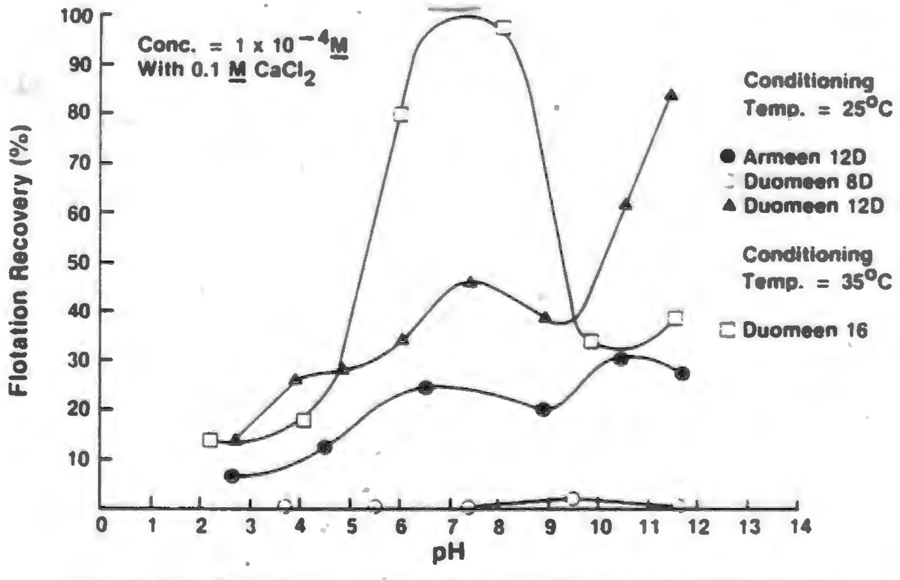

Figure 31b. Flotation recovery of magnetite as a function of pH.

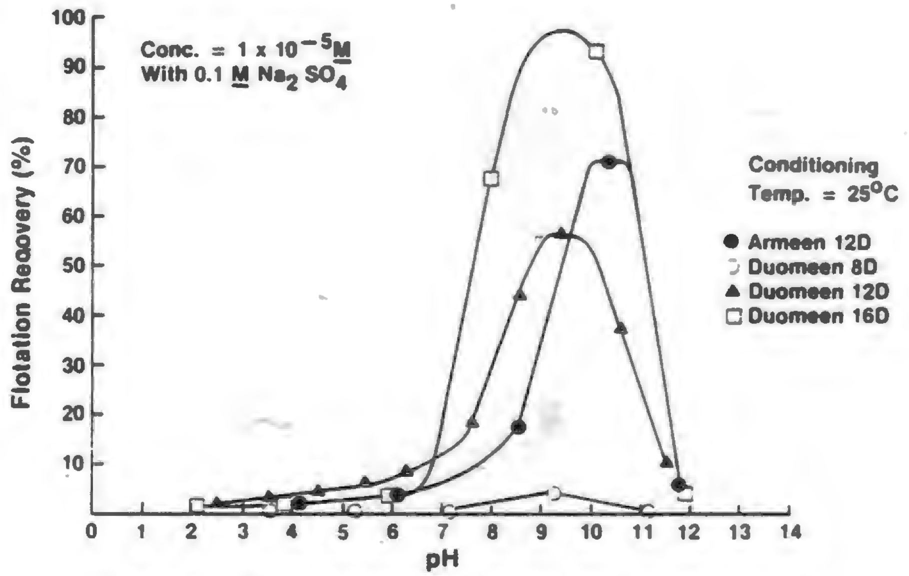

Figure 32a. Flotation recovery of quartz as a function of pH.

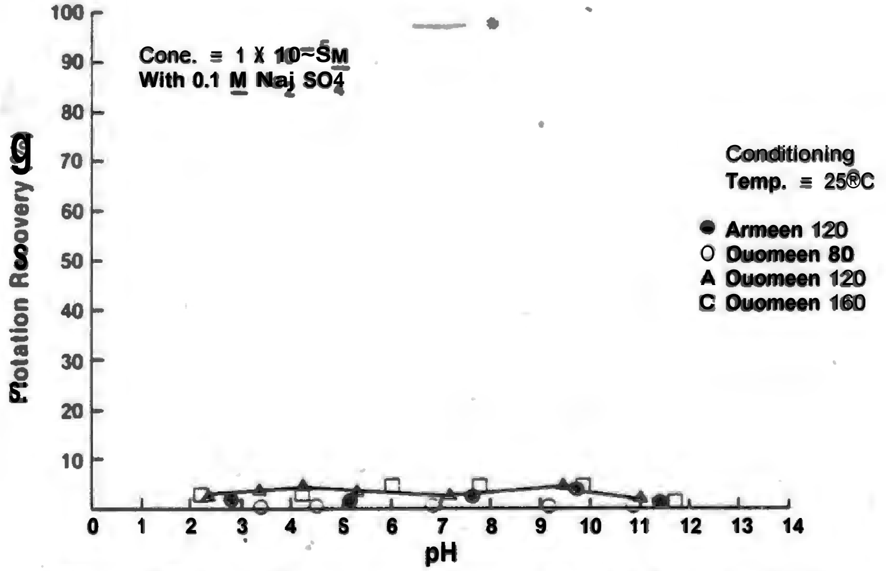

Figure 32b. Flotation recovery of magnetite as a function of pH.

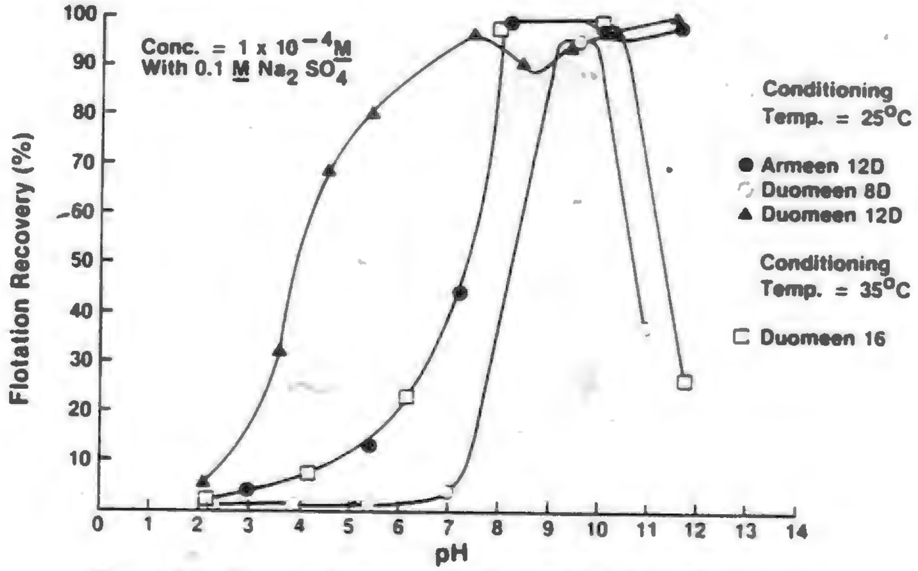

Figure 33a. Flotation recovery of quartz as a function of pH.

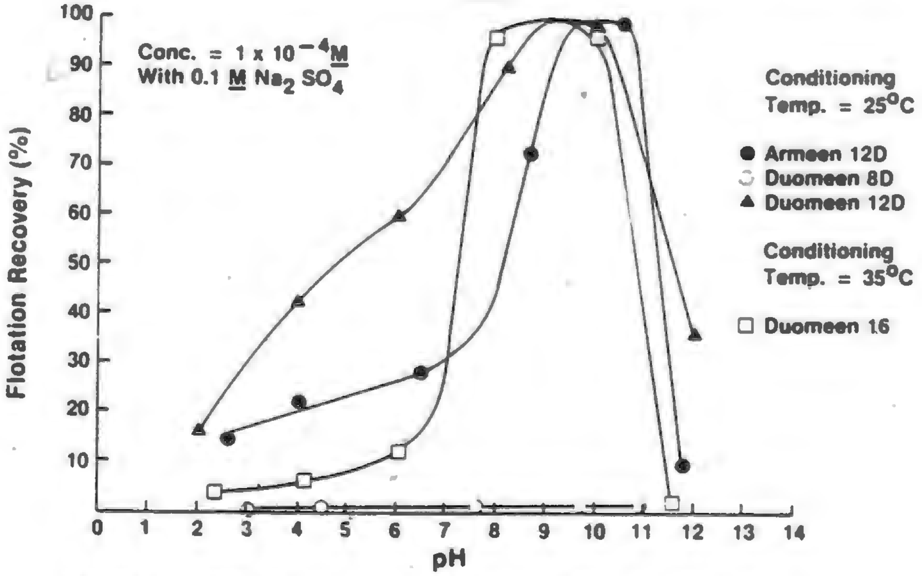

Figure 33b. Flotation recovery of magnetite as a function of pH.

DISCUSSION

In the present investigation, the pH of the pretreatment solution and the extent of crushing prior to pretreatment is demonstrated to have an important influence upon the flotation recovery of quartz. Depending upon the extent of crushing, acidic pretreatment solutions were observed to shift quartz flotation recovery curves in the alkaline direction. This decrease in quartz flotation recovery is caused by the charge reversal from positive to negative on the quartz surface, thereby producing repulsion of the positively charged polar heads of the collector ions. The shift in an oxide mineral's PZC is highly dependent upon pretreatment conditions (Kolarik, Dixon, Freeman, Furlong and Healy, 1980; Sandvik, and Solbakken, 1968).

The influence of an additional amino group was observed to be responsible for the increased flotation rate of quartz and magnetite. This conclusion is supported in part by the results of Bleir and co-workers (Bleir, Goddard and Kulkarni, 1976). It is felt that the additional 3-carbon chain separating the two amino groups contributes little, if anything, to this observed increase in quartz and magnetite flotation recovery. This conclusion is based on the fact that the Duomeen 8D compound, which has a total of 11 methylene groups, exhibits much poorer quartz and magnetite flotation recovery than the primary amine (12A), which has a hydrocarbon chain length of 12 methylene groups. Illustrations of this can be seen in Figures 26a through 33b.

Hydrocarbon association was also observed to be responsible for the increased flotation rate of quartz and magnetite, using 10^{-4} $\underline{M}$ rather than 10^{-5} $\underline{M}$ for the various amine compounds studied.

The significant role that pH has in determining the sign and magnitude of the oxide mineral surface charge is also illustrated in several quartz-magnetite flotation recovery curves that were obtained under the influence of ionic strength. For these curves, flotation recovery is poor over most of the pH range, except at the higher pH values (i.e., pH 9 to pH 12). This increase in flotation recovery is attributed to more strongly adsorbed collector ions on a highly negatively charged mineral surface. The large negative charge was imparted by the presence of hydroxyl ions at high pH.

The effect of pH was also observed to influence collector hydrolysis and, in turn, influence quartz and magnetite recovery. As has been seen, for both quartz and magnetite flotation systems, recovery is seen to drop off near pH 12. This is attributed to the fact that at this pH most of the collectors studied are in the form of neutral molecules which do not adsorb on the quartz and magnetite surfaces. It should be noted, however, that neutral molecules can act as excellent collectors when present with the ionic surfactant species (Fuerstenau and Yamada, 1962; Smith, 1963). For the quartz and magnetite systems studied containing an added salt(s), the presence of neutral amine molecules at high pH values would increase collector solubility, which would also increase the flotation rates of quartz and magnetite in these systems.

Comparing Figures 10a, 10b, 11a, 11b, and 13, it can be seen that quartz experimental samples which were crushed to -65 +150 mesh and then leached in concentrated hot HCl, gave the poorest quartz flotation recovery in the lower pH range. For this decrease in quartz flotation recovery, the quartz surface must have a highly charged positive surface (see Eq. 2). On the other hand, quartz crystals which were first leached and then crushed gave much better flotation recovery. Quartz samples which were stored in double-distilled water gave the best flotation recovery. For this increase in flotation recovery, the quartz surface must be negatively charged to promote collector attachment (see Eq. 1). On the basis of this behavior, there appears to be a correlation between the amount of collector adsorbed and quartz pretreatment sample size. It is evident that the quartz surface strives for equilibrium at a low pH, but can be shifted in either direction, depending on pretreatment conditions and extent of crushing. (This phenomenon man someday be useful in the separation of oxide minerals which differ in hardness but have close PZC's.) This is supported in part by the fact that quartz and magnetite collector systems (anionic or cationic) in the pH range 7 to 9 very rarely stabilize, in the sense that the final pH keeps shifting in the acidic direction in this pH range, and has been observed by the author to shift further to the left, depending on the particle size distribution. The finer size fraction, -65 +325 mesh, shifting more than the -65 +150 mesh fraction. This may be due to the differences of particle surface area reacting with a system in which the potential-determining ions are nearly equal in concentration. This shift in pH has also been observed by fellow researchers (Smith, Rajala, and Wei, 1982).

Depending on quartz pretreatment, and collector used, a trough and two flotation, and/or adsorption peaks were observed. These peaks corresponded to the observed pKa values for the 12D quartz-amine systems studied. Similar observations were also observed for the other quartz-magnetite amine systems studied. The first observed flotation peak for the quartz-12D systems were highly indicative of pretreatment conditions and 12D concentration. Whereas, quartz-12D adsorption systems (-65 +325 mesh) in the presence of collector solution only always showed this type of behavior. Illustrations of this can be seen in Figures 9, 10a, 11a, 11b, 12a and 12b.

It is interesting to note that the concentrations of the 12D ionic species in the pH range 6 to 8 are close in concentrations, with the +1 species predominating; (refer to Figure 3). Charge interaction of these collector species may account for the observed trough (decreased quartz flotation recovery). As was seen in Figures 5 through 9, variations in conditioning rpm and sample size considerably influenced diamine adsorption on quartz and magnetite. This behavior would suggest that the electrostatic forces within the double layer for quartz (and possibly magnetite) are weak and are sensitive to slight environmental changes. These electrostatic forces may be further influenced by the potential-determining ions (H^+ and OH^-), which are also close in concentration in the pH range pH 6 to pH 8. In some circumstances, this may result in decreased flotation recovery.

Another variable which may be responsible for the observed trough is the formation of the first hydroxy complex of Cu^{++}, which occurs in this pH range (Fuerstenau and Palmer, 1976). If a hydroxy complex were formed, either by Cu^{++} or some other metal ion, the quartz surface would become positively charged, and thus, repel a cationic collector. Based on the analysis of quartz and the care taken in mineral preparation, the formation ~~of~~ the first hydroxy complex of Cu^{++} does not seem likely. However, it may be possible that a synergistic effect is being seen. As was seen in Figures 10a, 10b, and 11a, pretreatment conditions had a considerable influence on quartz flotation recovery. Quartz crystals which were leached before crushing, or not at all, shifted flotation recovery to the lower pH values. This, coupled with the fact that the spectrographic analysis of quartz revealed 0.007 weight percent Cu, and that wet screening prior to drying was carried out in tyler brass screens in double-distilled water which was slightly acidic, may have been the combination that would cause this type of flotation behavior, or depression in this pH range.

The reason for stating this is that numerous attempts were made to try to duplicate this type of flotation response. The only successful attempt was when the 12D concentration was lowered to 10^{-6} $\underline{M}$ (Figure 11a), where the quartz crystals were first leached and then crushed to -65 +150 mesh, wet screened, dried and then floated. As was stated earlier, a hydroxy complex is very surface-active and has been observed to adsorb on positively-charged surfaces. Provided the PZC of quartz was not shifted in the alkaline direction, (as was seen in most of the quartz flotation recovery curves), the formation of the first hydroxy complex of Cu^{++} would indeed cause the observed troughs, or decreased quartz flotation rate seen in the above-mentioned figures.

The effect of ionic strength was observed to cause a reduction in quartz and magnetite flotation recovery, in most cases. This was attributed to the competition for surface sites between the various salt(s) and amine ions (Fuerstenau and Modi, 1960), and a decrease in collector solubility. As collector chain length and concentration were increased, a less pronounced reduction in quartz and magnetite flotation recovery was observed. This was attributed to the association of hydrocarbon chains. In general, sodium sulfate was found to have the least influence, sodium chloride the second most, and calcium chloride the most influence on quartz and magnetite flotation recovery. This behavior is supported by the results of Modi and Fuerstenau (Fuerstenau and Modi, 1960). Greater quartz and magnetite depression using 0.1 M $CaCl_2$ is credited to a stronger specific adsorption and a larger degree of competition with the collector ions. Illustrations of this can be seen in Figures 15a, 16a, 18a, 18b, 20a, and 23b.

In some cases, sodium sulfate and calcium chloride were observed to act as mild activators for quartz and magnetite in the lower pH range. Illustrations of this can be seen in Figures 19a, 21a, 21b, 22a, 22b, 23b, and 24b. It is interesting to note that quartz and magnetite activation is only observed for the 12-carbon amine quartz-magnetite systems. This is assumed to be due to differences in collector solution properties exhibited by this compound, and in the case of quartz, possible shifts in its PZC due to pretreatment variations, resulting from independent batch preparations.

For activation to occur in electrostatic systems, the electrical double layer must become crowded with counter-ions to the point that the particle surface becomes highly negative, and thus, provides the means for electrostatic attraction of the 12D collector ions. This can only occur when the divalent counter-ions are oppositely charged to the collector and the mineral surface species (Somasundaran, 1975).

The influence of micelle formation on flotation depression at 0.6 M NaCl, 0.1 M $CaCl_2$, and 0.1 M Na_2SO_4, is of little consequence, since none of the reported CMC's were reached (Table 1). However, the lower the ionization constant and solubility, the lower will be the maximum pH of flotation (Smith, 1973).

Illustrations of this phenomenon are clearly evident in Figures 26a and 26b. As can be seen, an increase in collector chain length shifts the pH of maximum flotation to the lower pH values. It is also noteworthy that the 12-carbon primary amine (12A) has a slightly higher pH of maximum flotation recovery than the 12D amine, for both quartz and magnetite. Because the 12A compound is a stronger base, and thus has a higher ionization constant than the corresponding 12D compound, a shift toward the higher pH range is observed. The pH of maximum flotation is also observed to correspond to the pKa value noted for this compound.

Slightly poorer recoveries were observed for quartz and magnetite when their pulps were conditioned at 75°C, using 10^{-4} $\underline{M}$ 12D and 12A. This is probably because the amine compounds begin to break down in this temperature range. (Refer to Armak Chemical Co. Amine literature.) However, Somasundaran suggests that a decrease in flotation recovery is characteristic of electrostatic systems as temperature is increased, where bond energies are low, and that the reverse is true for chemisorption systems (Somasundaran, 1975).

Comparing Figures 21a, 21b, 22a, 22b, 23a, 23b, 24a, and 24b, it is interesting to note that the observed decrease in quartz and magnetite flotation recovery occurs primarily in the lower pH range.

Comparison of the flotation curves in Figures 26a through 33b shows that, in general, Duomeen 16 is a much better collector for quartz and magnetite than 8D, 12D and

12A are. Obviously, Duomeen 16 is adsorbed much more strongly at the solid-liquid interface, and possibly, air-water interface than the shorter-chained amine compounds.

The magnetite-amine systems studied are influenced to a greater extent by the additions of the various salts than the corresponding quartz-amine systems are. Because of this phenomenon, a high-grade magnetite concentrate from silica is possible, provided flotation is carried out at a low pH and low collector concentration. Once the adsorption potential of the amine is increased through an increase in concentration or chain length, this separation is not possible.

SUMMARY AND CONCLUSIONS

Hallimond tube microflotation studies and picric acid adsorption studies were conducted to determine the effects of -- mineral pretreatment conditions, ionic strength, an additional amino group, collector chain length, and conditioning temperature -- on flotation recoveries of quartz and magnetite.

Sodium chloride, anhydrous calcium chloride, and sodium sulfate were the three salts used to control ionic strength.

The four cationic collectors studied were 8D, 12D, 12A and Duomeen 16 -- all members of the alkyl amine group.

Pretreatment pulp temperatures were 25°C, 35°C (for Duomeen 16 only) and 75°C.

From the results of this investigation, the following conclusions can be made:

1) The adsorption of 12D on quartz drops off as conditioning rpm increases from 0 to 180 rpm.

2) The extent of crushing prior to pretreatment adversely affects 12D and 12A quartz flotation recoveries in the lower pH range. Quartz crystals pretreated with HCl prior to crushing give better flotation recoveries than quartz crystals which are first crushed and then pretreated. Quartz crystals which are first crushed and then pretreated with double-distilled water only, give much better flotation recoveries in the lower pH range, as compared with the other two pretreatment methods noted above.

3) Depending on quartz pretreatment conditions, the pH's of maximum quartz flotation recoveries correspond to the respective pKa values noted for the Duomeen 12D compound in systems without any salt addition. Similar observations were made for the other amine systems studied.

In some cases, two flotation and/or adsorption peaks separated by a trough appear in the pH range from about pH 6.5 to pH 8.5. The exact nature of this decrease (trough) in quartz flotation recovery and in quartz 12D adsorption curves is not clear at this time, but may be attributed to one or more of the following: charge interaction of the amine species in this pH range; the formation of the first hydroxy complex of Cu^{2+}; or weak electrostatic forces sensitive to slight environmental changes.

4) Without any salt addition, longer-chained alkyl amines give better flotation recoveries of quartz and magnetite.

5) In general, flotation of quartz and magnetite with Duomeen 12D is greater than with the corresponding primary amine 12A, for the systems studied. This is primarily attributed to the presence of the additional amino group for the 12D compound. The influence of the three additional carbons separating the two amino groups appears to contribute little, if anything, to the increase in quartz flotation. At high preconditioning temperatures (75°C), quartz and magnetite flotation recoveries (12D and 12A systems) were decreased, as compared with the same systems preconditioned at 25°C.

6) At low preconditioning temperatures, flotation of quartz or magnetite with 10^{-5} M 8D, 12D, 12A and Duomeen 16 is adversely affected by the addition of 0.6 M NaCl, 0.1 M $CaCl_2$ and 0.1 M Na_2SO_4. In comparison, quartz and magnetite flotation is greater with Duomeen 16 than with the shorter-chained amines. Once the amine collector concentrations are increased to 10^{-4} M, a noticeable increase in flotation recovery for all systems is observed. In general, Na_2SO_4 has the least influence, NaCl the second least, and $CaCl_2$, the most influence on quartz and magnetite depression.

7) The mechanism of depression by NaCl, $CaCl_2$ and Na_2SO_4 on the flotation of quartz and magnetite with 8D, 12D and 12A appears to be ion competition for adsorption sites in the electrical double layer. Depression of quartz and magnetite by $CaCl_2$ in the basic pH range is credited to the specific adsorption of Ca^{++} and $CaOH^+$, as well as a decrease in amine solubility. For the 12D systems, SO_4^{2-} is seen to act as a mild activator for both quartz and magnetite in the lower pH range. For recovery of quartz and magnetite with Duomeen 16, the mechanisms of depression by the same salts appear to be collector solubility, CMC-lowering, and ion competition. At high pH values, collector solubility seems to be the dominant mechanism, especially for pulps containing $CaCl_2$.

8) With no salt additions, the maximum pH of flotation for quartz and magnetite is greater using the primary amine 12A than it is using the diamines 8D, 12D and Duomeen 16. This is due to lower collector solubilities and ionization constants.

RECOMMENDATIONS FOR FUTURE RESEARCH

Other experimental techniques which would aid in substantiating the adsorption-flotation results follow:

Electrokinetic studies using a Zeta Meter on quartz particles which are pretreated in acidic, neutral and alkaline solutions could be done. Investigations of this nature would elucidate some of the collector-mineral adsorption mechanisms.

Surface tension experiments (i.e., capillary rise) at different temperatures and salt concentrations could also be conducted. These measurements would reflect some of the collector adsorption mechanisms occurring at the air-solution interface.

Collector solubilities at different temperatures and salt concentrations should also be measured in order to determine the "solubility effect" upon flotation rates.

Adsorption and micro-flotation studies could be conducted in increasing ionic strength solutions, at different conditioning times and temperatures from the ones previously used.

Variations in mineral pretreatment, with regard to particle size should also be examined.

Finally, contact angle studies could be conducted. These studies should reflect the degree of hydrophobicity of these systems and aid in correlating adsorption and micro-flotation studies.

BIBLIOGRAPHY

Adamson, A. W., *Physical Chemistry of Surfaces*. 3rd Ed., Interscience Publishers, New York. p. 209; 1976.

Aplan, F. F. and Fuerstenau, D. W., *Froth Flotation*. 50th Anniversary Volume, Fuerstenau, D. W. Editor, (AIME), New York. p. 170; 1962.

Bleir, A., Goddard, E. D., and Kulkarni, R. D., *Flotation*. A. M. Gaudin Memorial Volume, Fuerstenau, M. C. Editor, (AIME), New York. vol. 1, pp. 126-138; 1976.

Dayton, S. L., et al., "Engr. and Mining J.". 181, p. 115; 1980.

de Bruyn, P. L., *Trans. AIME*. vol. 202, p. 291; 1955.

Fuerstenau, D. W. and Modi, H. J. J., *Electrochem. Soc*. vol. 106, p. 336; 1959.

Fuerstenau, D. W. and Modi, H. J., *Trans. AIME*. vol. 217, p. 381; 1960.

Fuerstenau, D. W., Ed., *Froth Flotation*. 50th Anniversary Volume, (AIME), New York. pp. 182-185, and 105-106; 1962.

Fuerstenau, D. W. and Yamada, B. J., *Trans. AIME*. vol. 223, p. 50; 1962.

Fuerstenau, D. W., Healy, T. W. and Somasundaran, P., *Trans. AIME*. vol. 229, p. 321; 1964.

Fuerstenau, M. C. and Palmer, B. R., *Flotation*. Gaudin Memorial Volume, Fuerstenau, M. C. Editor, (AIME), New York. vol. 1, p. 148; 1976.

Gaudin, A. M. and Morrow, J. G., *Trans. AIME*. vol. 199, p. 1196; 1954.

Gaudin, A. M. and Fuerstenau, D. W., *Trans. AIME*. vol. 202, p. 66; 1955.

Gaudin, A. M. and Fuerstenau, D. W., "Quartz Flotation with Cationic Collectors". *Trans AIME*. vol. 202, pp. 958-962; 1955.

Healy, T. W. and Fuerstenau, D. W., *J. Colloid Sci*. vol. 20, p. 376; 1955.

Iwasaki, I., Cooke, S. R. B. and Kim, Y. S., Trans. AIME. vol. 223, p. 113; 1962.

Kolarik, L. O., Dixon, D. R., Freeman, P. A., Furlong, D. N. and Healy, T. W., Fine Particles Processing (AIME). vol. 1, Ch. 34; 1980.

Kruyt, H. R., Colloid Science I. Ch. 4, 5, Elsevier Publishing Co., New York. 1952.

Kulkarni, R. D., and P. Somasundaran, paper presented at 164th meeting of Am. Chem. Soc., New York (1972).

Kulkarni, R. D. and Somasundaran, P., Trans. AIME. vol. 262, p. 120; 1977.

Li, H. C., Adsorption of Inorganic and Organic Ions on Quartz. ScD. Thesis, Massachusetts Inst. of Technology; 1957.

Onoda, G. Y., and Fuerstenau, D. W., VII International Mineral Processing Congress. vol. I, Gordon and Breach, New York. p. 301; 1964.

Parks, G. A., Chem. Rev. vol. 65, p. 197; 1965.

Rajala, J. A., The Effects of Increasing Ionic Strength, Collector Chain Length, and Temperature on Anionic Flotation of Oxide Minerals. M. S. Thesis, Univ. of Nev., Reno; 1981.

Ralston, A. W., Fatty Acids and Their Derivatives. John Wiley and Sons, Inc., New York. p. 378; 1948.

Sandvik, K. L. and Solbakken, A., Trans. AIME. vol. 241, pp. 419-420; 1968.

Shinoda, K., Colloidal Surfactants. Hutchinson, E. and Van Rysselberghe, P. Editors, Academic Press, New York. p. 1; 1963.

Smith, R. W., Trans. AIME. vol. 226, pp. 427-433; 1963.

Smith, R. W., Trans. AIME. vol 254, pp. 353-357; 1973.

Smith, R. W. and Akhtar, S., Flotation. A. M. Gaudin Memorial Volume, Fuerstenau, M. C. Editor, (AIME), New York. vol. 1, pp. 82-116; 1976.

Smith, R. W. and Chini, J., NSF grant, Univ. of Nev., Reno, Personal Communication; 1980.

Smith, R. W., and McGill, S., NSF grant, Univ. of Nev., Reno, Personal Communication; 1981.

Smith, R. W., Rajala, J. A. and Wei, Univ. of Nev., Reno, Personal communication; 1981.

Smith, R. W., Univ. of Nev., Reno, Personal communication; 1982.

Somasundaran, P., and Kulkarni, R. D., Trans. IMM. London. 82, C163; 1973.

Somasundaran, P., Interfacial Chemistry of Particulate Flotation, AIChE. vol. 71, No. 150; 1975.

Stigter, D., and Overbeek, J. Th. G. Proceedings of the Second International Congress on Surface Activity. vol. I., Butterworth's, London. p. 311; 1958.

C′

APPENDIX I

Results reported for Figures 5 through 33b

Figure 5

Adsorption (moles x 10^8
per gram quartz)

open circle

moles	pH
0.0	2.25
10.0	3.40
48.0	4.00
61.0	4.80
60.0	5.46
10.0	5.93
0.0	6.70
98.0	6.91
20.0	7.41
50.0	8.55
70.0	9.71
48.0	10.00
66.0	10.48
20.0	11.17
0.0	11.25

Adsorption (moles x 10^8
per gram quartz)

closed circle

moles	pH
40.0	2.25
46.0	3.30
62.0	4.38
100.0	5.60
63.0	6.45
68.0	7.70
34.0	9.35

34.0	10.20
134.0	11.35
74.0	11.90

Figure 6

Adsorption (moles x 10^8
per gram quartz)

moles	Conditioning rpm
82.0	0
84.0	60
52.0	120
34.0	180

Figure 7

Adsorption (moles x 10^8
per gram magnetite)

moles	pH
34.0	2.25
40.0	4.33
30.0	6.10
34.0	9.10
74.0	11.00

Flotation recovery (%)	pH
10.8	2.51
24.2	3.45
25.4	4.45
32.2	5.44
45.2	6.44
89.4	7.45
89.7	8.72
98.5	10.57
97.0	9.45
96.4	11.55

Figure 8

Adsorption (moles x 10^8 per gram quartz) moles	Log conc. of unadsorbed Duomeen 12D
1.9	9.81×10^{-7} M
24.0	9.76×10^{-6} M
0.0	5.00×10^{-5} M
19.1	4.98×10^{-5} M
257.0	9.74×10^{-5} M
370.0	4.96×10^{-4} M
490.0	9.95×10^{-4} M

Figure 9

Adsorption (moles x 10^8
per gram quartz)

closed triangle

moles	pH
0.0	2.30
200.0	4.66
400.0	5.50
300.0	5.95
0.0	6.45
200.0	7.00
140.0	7.42
370.0	8.65

Adsorption (moles x 10^8
per gram quartz)

open circle

moles	pH
0.0	2.35
20.0	3.40
40.0	4.00
60.0	4.60

60.0	4.80
80.0	4.95
120.0	5.10
140.0	5.55
40.0	6.45
40.0	7.20
40.0	7.95
40.0	8.40
160.0	9.55
140.0	9.65
100.0	10.45
60.0	11.05
40.0	11.85

Figure 10a

Flotation recovery (%)	pH
open circle	
4.0	2.17
22.1	2.98
65.1	3.97
83.2	5.16
90.3	6.35
90.0	7.04
94.2	7.88
closed circle	
3.1	2.18
7.2	3.20
50.7	4.15
74.6	5.08
85.6	5.75
80.6	6.65
55.2	7.75
96.3	8.55

open square

2.3	2.24
10.5	3.00
43.3	3.99
59.2	4.80
84.8	5.85
91.8	6.54
93.7	7.13
95.1	7.67
98.2	8.65

closed triangle

5.5	4.32
29.1	5.45
20.2	5.53
54.0	5.95
72.3	6.48
82.3	7.11
88.7	7.15
91.1	7.50
92.0	8.00
98.5	8.70

Figure 10b

open circle

Flotation recovery (%)	pH
0.7	1.98
5.3	3.10
14.2	3.95
54.6	5.25
91.9	6.02
96.1	6.85
96.1	8.00
97.9	8.93

open square

0.8	2.85
4.5	4.45
33.2	5.45
95.0	7.85
100.0	10.25

Figure 11a

Flotation recovery (%)	pH
open circle	
3.6	1.98
26.7	3.50
96.2	5.47
94.7	7.51
100.0	9.33
100.0	11.34
open square	
3.1	2.18
7.2	3.20
50.7	4.15
74.6	5.08
85.6	5.75
80.6	6.65
55.2	7.75
96.3	8.55
91.5	9.25
95.9	9.95
95.7	10.93
25.9	11.95
closed triangle	
5.5	4.32
29.1	5.45
20.2	5.53
72.2	6.48
91.1	7.50

98.5	8.70
99.2	9.68
95.2	10.40
89.0	11.53

closed circle

5.9	4.43
42.1	5.68
61.7	6.10
49.3	6.93
57.5	7.64
78.9	9.06
18.3	9.90
5.8	11.20

Figure 11b

Adsorption (moles x 10^8
per gram quartz)

open circle

moles	pH
0.0	2.35
20.0	3.40
40.0	4.00
60.0	4.60
60.0	4.80
80.0	4.95
120.0	5.10
140.0	5.55
40.0	6.45
40.0	7.20
40.0	7.95
40.0	8.40
160.0	9.55
140.0	9.65
100.0	10.45
60.0	11.05
40.0	11.85

closed triangle

0.0	2.25
0.8	4.10
2.4	4.98
1.6	5.48
0.6	5.95
0.6	7.86
2.6	9.00
2.2	9.86

Figure 12a

Flotation recovery (%)	Log Concentration (12D)
open circle - pH 5.5	
58.1	1×10^{-6} M
82.8	5×10^{-6} M
89.0	1×10^{-5} M
99.1	5×10^{-5} M
99.5	1×10^{-4} M
99.6	5×10^{-4} M
99.1	1×10^{-3} M
open square - pH 7.5	
42.9	1×10^{-6} M
90.9	5×10^{-6} M
95.4	1×10^{-5} M
97.8	5×10^{-5} M
99.6	1×10^{-4} M
99.6	5×10^{-4} M
99.5	1×10^{-3} M
closed triangle - pH 9.5	
59.6	1×10^{-6} M
97.5	5×10^{-6} M
98.7	1×10^{-5} M
97.7	5×10^{-5} M
96.7	1×10^{-4} M

99.7	5×10^{-4} M
99.6	1×10^{-3} M

Figure 12b

Adsorption (moles x 10^{8} per gram quartz) moles	Log concentration of unadsorbed 12D mole~~s~~/liter
open circle - pH 5.5	
0.6	9.93×10^{-7}
0.8	4.99×10^{-6}
1.3	9.99×10^{-6}
5.0	4.99×10^{-5}
23.1	9.98×10^{-5}
49.9	4.99×10^{-4}
57.6	9.99×10^{-4}
open square - pH 7.5	
0.0	1.00×10^{-6}
2.0	4.98×10^{-6}
1.7	9.98×10^{-6}
4.5	4.99×10^{-5}
13.5	9.99×10^{-5}
23.1	4.99×10^{-4}
55.7	9.99×10^{-4}
closed triangle - pH 9.5	
1.1	9.89×10^{-7}
1.6	4.98×10^{-6}
8.4	9.92×10^{-6}
16.6	4.98×10^{-5}
61.5	9.94×10^{-5}
103.7	4.99×10^{-4}
107.6	9.99×10^{-4}

Figure 13

Flotation recovery (%)	pH
open square	
3.6	2.15
27.3	3.51
97.3	5.55
98.5	7.42
90.9	9.45
88.3	9.85
96.3	11.64
closed circle	
5.6	2.44
8.2	4.35
66.0	5.24
86.2	6.00
98.9	7.35
96.0	9.43
97.1	10.33
99.0	11.74
open circle	
5.2	2.52
14.9	4.50
54.5	6.46
67.8	8.71
97.1	10.51
18.0	11.75
closed triangle	
1.4	3.98
10.4	6.10
49.8	8.31
98.1	10.51
20.0	11.75

Figure 14

Flotation recovery (%)	pH
open circle	
8.3	2.14
25.1	4.04
97.6	6.02
98.2	7.94
93.4	9.88
88.5	11.42
closed triangle	
5.7	2.13
20.6	4.00
92.5	6.00
97.5	7.98
96.4	9.83
72.8	11.42

Figure 15a

Flotation recovery (%)	pH
no additions	
0.0	2.92
2.3	5.34
11.8	7.24
91.2	9.51
59.2	11.02
with 0.6 M NaCl	
0.0	3.31
0.0	6.21
0.0	8.54
0.01	9.85
0.0	11.65

with 0.1 $\underline{M}$ $CaCl_2$	
0.0	3.10
0.0	5.50
0.0	7.81
0.0	9.28
0.0	11.21
with 0.1 $\underline{M}$ Na_2SO_4	
0.0	3.52
0.5	5.43
0.9	7.12
4.6	9.25
0.0	11.22

Figure 15b

Flotation recovery (%)	pH
no additions	
0.0	3.31
0.2	5.53
0.5	7.79
8.8	9.56
1.5	11.28
with 0.6 $\underline{M}$ NaCl	
0.0	3.40
0.0	5.34
0.0	7.59
0.0	9.36
0.0	11.27
with 0.1 $\underline{M}$ $CaCl_2$	
0.0	3.70
0.0	5.90
0.0	7.83
0.0	9.21
0.0	11.50

with 0.1 M Na_2SO_4

0.0	3.16
0.1	4.54
0.0	6.85
1.4	9.29
0.0	10.93

Figure 16a

Flotation recovery (%)	ph
no additions	
5.5	4.32
20.2	5.45
29.1	5.45
54.5	5.93
72.3	6.48
82.0	7.11
88.5	7.19
91.1	7.50
92.0	8.00
98.5	8.70
99.2	9.68
95.2	10.40
89.0	11.53
with 0.6 M NaCl	
4.4	1.98
4.6	2.95
4.2	3.98
5.1	5.05
8.6	6.00
12.8	7.13
30.7	8.35
57.9	9.17
37.2	10.15
5.4	11.08
1.7	11.95

with 0.1 $\underline{M}$ $CaCl_2$

2.1	2.13
2.1	3.05
3.2	4.20
7.8	5.13
7.9	6.05
17.2	7.35
33.8	8.30
27.3	9.00
8.6	10.13
8.1	11.40

with 0.1 $\underline{M}$ Na_2SO_4

2.3	2.55
3.4	3.53
4.8	4.45
5.9	5.45
8.2	6.30
18.9	7.55
43.7	8.65
55.8	9.35
37.3	10.55
10.3	11.50

Figure 16b

Adsorption (moles x 10^8
per gram quartz)

moles	pH
	no additions
0.0	2.25
0.8	4.10
2.4	4.98
1.6	5.48
0.6	5.95
0.6	7.86
2.6	9.00
2.2	9.86

with 0.6 M NaCl

0.3	3.80
0.6	6.33
1.3	8.55
2.8	9.15
3.4	10.36
1.2	11.43

with 0.1 M $CaCl_2$

0.2	3.15
1.0	4.98
1.4	7.05
1.6	8.15
3.0	9.30
0.6	10.68

with 0.1 M Na_2SO_4

0.5	4.25
0.7	5.95
0.9	8.20
2.5	9.20
3.0	10.50

Figure 17a

Flotation recovery (%)	pH
no additions	
2.9	2.60
3.8	3.45
4.7	4.47
5.4	5.40
6.9	6.40
14.2	7.65
30.1	8.65
40.3	9.45
16.7	10.52
1.5	11.50

with 0.6 M NaCl	
1.3	2.80
1.7	3.85
1.5	5.36
2.6	6.36
2.4	7.73
3.5	8.75
2.5	9.33
0.9	10.32
with 0.1 M $CaCl_2$	
2.7	4.10
4.3	4.97
2.7	6.05
2.5	7.75
4.0	8.55
1.3	9.92
with 0.1 M Na_2SO_4	
2.3	2.25
2.7	3.25
3.7	4.25
2.7	5.25
3.3	7.15
1.4	9.35
4.4	10.95

Figure 17b

Adsorption (moles x 10^8 per gram magnetite)

moles	pH
no additions	
0.6	3.90
0.4	6.73
1.4	8.15
4.1	9.50
0.0	10.83

with 0.6 $\underline{M}$ MaCl

0.0	3.85
0.0	8.23
0.0	10.05

with 0.1 $\underline{M}$ $CaCl_2$

0.0	4.14
0.0	6.05
0.0	9.05

with 0.1 $\underline{M}$ Na_2SO_4

0.0	4.50
0.0	7.35
0.0	10.21

Figure 18a

Flotation recovery ***a)***	pH
	no additions
1.4	3.98
10.4	6.10
49.8	8.31
98.1	10.61
20.0	11.75
	with 0.6 $\underline{M}$ NaCl
1.0	3.50
4.1	6.31
3.6	7.53
13.6	8.51
18.6	9.84
8.6	10.37
2.9	11.52
	with 0.1 $\underline{M}$ $CaCl_2$
1.6	3.62
1.9	6.55
10.7	8.64

6.1	10.42
6.9	11.53

with 0.1 M Na_2SO_4

1.8	4.11
3.7	6.15
18.1	8.54
71.3	10.29
6.7	11.75

Figure 18b

Flotation recovery (%)	pH
no additions	
0.5	4.60
3.3	6.55
4.4	8.35
27.4	9.41
12.2	10.51
1.0	11.73
with 0.6 M NaCl	
0.0	2.53
0.5	4.60
0.7	6.42
0.9	8.45
1.5	10.41
0.4	11.72
with 0.1 M $CaCl_2$	
0.0	2.40
0.2	4.45
0.5	6.51
0.7	8.32
0.7	10.56
0.1	11.65

with 0.1 $\underline{M}$ Na_2SO_4

0.3	2.71
0.5	5.12
0.7	7.63
0.9	8.71
1.4	10.45
0.6	11.69

Figure 19a

Flotation recovery (%)	pH

no additions

9.9	2.12
82.9	3.93
95.7	6.02
98.3	7.40
95.3	9.75
55.9	11.73

with 0.6 $\underline{M}$ NaCl

0.7	2.15
8.3	3.75
59.6	5.92
98.4	8.00
95.8	10.05
44.0	11.65

with 0.1 $\underline{M}$ $CaCl_2$

1.8	2.10
1.6	3.95
2.6	5.95
67.4	8.00
93.4	10.12
4.1	11.88

with 0.1 $\underline{M}$ Na_2SO_4

2.3	2.1
3.2	4.15

3.8	6.00
4.4	7.75
4.0	9.85
1.5	11.65

Figure 19b

Flotation recovery (%)	pH

no additions

3.0	1.95
4.4	3.95
7.8	5.93
22.8	7.00
38.2	8.15
57.6	8.85
6.6	9.92
5.2	10.05
1.5	11.73

with 0.6 M NaCl

3.4	2.00
3.3	4.02
4.3	6.45
9.1	8.00
8.5	9.35
3.3	11.00

with 0.1 M $CaCl_2$

3.4	2.25
4.2	4.67
5.1	7.75
2.7	9.85
1.9	11.55

with 0.1 M Na_2SO_4

2.3	2.10
3.2	4.15
3.8	6.00
4.4	7.75

4.4	9.85
1.5	11.65

Figure 20a

Flotation recovery (%)	pH
no additions	
0.6	3.00
12.5	5.18
39.8	6.41
97.5	7.99
99.1	9.00
99.0	10.85
10.5	12.06
with 0.6 M NaCl	
0.8	1.97
0.9	3.42
2.1	5.33
30.4	7.72
72.3	9.42
3.3	11.33
with 0.1 M $CaCl_2$	
0.0	2.13
1.1	5.03
11.7	7.72
16.4	9.11
5.1	10.39
11.3	11.71
with 0.1 M Na_2SO_4	
0.3	2.21
0.4	3.83
1.8	5.37
4.5	6.94
95.4	9.52
37.5	10.91

Figure 20b

Flotation recovery (%)	pH
no additions	
0.0	3.24
0.6	5.22
3.0	7.72
37.2	9.49
7.6	11.41
with 0.6 M NaCl	
0.0	3.31
0.7	5.22
0.7	6.98
1.5	9.30
0.8	11.40
with 0.1 M $CaCl_2$	
0.0	3.70
0.7	5.51
1.0	7.43
2.3	9.53
0.8	11.52
with 0.1 M Na_2SO_4	
0.4	4.50
0.3	5.80
0.7	7.67
1.5	9.58
0.2	10.91

Figure 21a

Flotation recovery (%)	pH
no additions	
0.7	1.98
5.3	3.10
14.2	3.95
54.6	5.25

91.9	6.02
96.0	6.85
96.1	8.00
97.9	8.93
98.2	10.00
99.0	10.93
100.0	12.22

with 0.6 M NaCl

- 4.5	2.23
5.3	3.12
13.1	4.17
25.6	5.15
59.7	6.28
97.6	7.34
96.0	8.16
91.3	9.33
99.9	10.25
100.0	11.00
96.5	11.95

with 0.1 M $CaCl_2$

5.0	2.11
11.4	3.17
37.2	4.12
61.5	5.10
81.3	6.15
96.9	7.25
94.1	8.35
92.8	9.24
96.7	10.05
98.7	10.95
98.7	11.95

with 0.1 $\underline{M}$ Na_2SO_4

4.4	2.15
32.7	3.45
68.2	4.50
79.9	5.45
88.5	6.35
95.7	7.40
91.0	8.35
93.2	9.35
97.5	10.35
99.8	11.50

Figure 21b

Flotation recovery (%)	pH
no additions	
10.8	2.51
24.2	3.45
25.4	4.45
32.2	5.44
45.2	6.44
89.4	7.45
89.7	8.72
97.0	9.45
98.5	10.57
96.4	11.55
with 0.6 $\underline{M}$ NaCl	
8.0	2.00
27.8	4.05
35.3	6.05
80.8	7.90
99.0	10.00
18.8	11.85
with 0.1 $\underline{M}$ $CaCl_2$	
13.4	2.72
25.9	3.90

27.9	4.90
34.5	6.08
46.1	7.38
38.7	8.92
61.7	10.50
83.6	11.45

with 0.1 M Na_2SO_4

15.8	2.05
41.1	4.05
59.1	6.00
89.5	8.25
97.5	9.95
35.4	11.95

Figure 22a

Flotation recovery (%)	pH
no additions	
2.4	2.18
5.0	3.55
35.4	5.11
30.1	5.45
99.4	6.75
99.2	8.00
96.2	9.26
98.7	10.37
99.8	11.92
with 0.6 M NaCl	
3.5	2.02
4.7	3.84
12.8	5.51
51.5	6.78
99.6	8.25
99.4	9.28
99.8	10.25
98.8	11.45

with 0.1 $\underline{M}$ $CaCl_2$

4.8	2.20
7.5	3.85
20.6	5.35
97.8	6.98
98.9	8.24
96.3	9.32
97.2	10.31
54.9	11.62

with 0.1 $\underline{M}$ Na_2SO_4

6.0	2.51
7.6	3.90
15.1	5.25
36.7	6.52
98.1	7.78
98.0	9.38
98.0	10.38
99.6	11.75

Figure 22b

no additions

Flotation recovery (%)	pH
3.1	2.22
7.4	3.45
7.9	5.05
29.5	6.42
97.3	8.18
96.1	9.25
98.4	10.35
55.0	11.83

with 0.6 $\underline{M}$ NaCl

3.9	1.97
12.7	3.78
15.1	4.91
24.1	6.25

62.6	7.75
77.6	9.02
27.3	9.28
88.4	10.35
15.3	11.62
With 0.1 M $CaCl_2$	
4.1	2.18
12.8	4.43
16.7	6.13
27.1	7.92
19.7	9.23
18.0	9.98
24.1	11.72
with 0.1 M Na_2SO_4	
4.4	2.52
9.5	3.56
16.5	5.14
29.6	7.23
75.1	8.15
96.8	9.38
99.2	10.32
33.6	11.73

Figure 23a

Flotation recovery (%)	pH
no additions	
4.8	2.82
54.6	5.21
98.7	6.63
98.7	8.55
93.7	10.18
91.2	11.35
with 0.6 M NaCl	
4.4	3.10
9.6	5.21

26.4	6.51
97.0	7.75
97.8	9.61
77.5	11.41

with 0.1 M $CaCl_2$

5.0	3.81
33.8	6.01
98.7	8.03
97.5	9.81
95.3	11.43

with 0.1 M Na_2SO_4

4.3	2.99
13.2	5.41
44.2	7.19
98.3	8.11
97.5	10.01
98.04	11.61

Figure 23b

Flotation recovery (%)	pH
no additions	
6.7	2.51
11.3	4.55
22.6	6.35
80.5	8.32
96.5	10.55
26.4	11.85
with 0.6 M NaCl	
9.7	2.52
19.5	4.57
25.6	6.40
63.0	8.45
75.6	10.35
6.6	11.57

with 0.1 M $CaCl_2$

6.8	2.55
12.6	4.34
24.4	6.42
20.2	8.80
30.7	10.37
27.8	11.65

with 0.1 M Na_2SO_4

14.1	2.62
21.5	4.53
28.7	6.53
72.7	8.62
99.3	10.53
9.3	11.73

Figure 24a

Flotation recovery (%)	pH
no additions	
5.2	2.32
4.6	3.69
48.4	5.38
95.5	6.63
100.0	7.62
99.6	9.16
85.9	9.62
97.3	10.40
96.5	11.92
with 0.6 M NaCl	
5.7	2.40
5.9	3.75
9.0	5.22
13.4	6.42
91.3	7.59
98.9	8.50

98.3	9.28
97.9	10.42
80.4	11.71

with 0.1 M $CaCl_2$

5.6	2.23
5.9	4.32
22.9	5.68
35.1	6.91
99.6	8.02
99.6	9.28
100.0	10.21
40.9	11.75

with 0.1 M Na_2SO_4

4.1	2.26
4.9	4.25
7.8	5.52
21.0	6.74
41.5	7.65
99.6	9.16
99.5	10.31
98.8	11.79

Figure 24b

Flotation recovery (%)	pH
no additions	
9.4	2.95
11.7	5.33
26.8	6.14
58.0	7.41
79.5	8.15
95.2	9.22
97.7	10.43
20.7	11.81

with 0.6 M NaCl

8.4	2.65
20.1	4.87
24.7	6.57
31.4	7.41
66.7	8.32
60.9	9.15
57.0	10.25
3.9	11.68

with 0.1 M $CaCl_2$

4.5	2.34
18.9	4.65
21.3	5.73
25.4	6.88
26.0	8.22
21.2	9.43
19.8	10.44
5.2	11.71

with 0.1 M Na_2SO_4

1.7	2.45
17.8	3.86
25.6	5.61
29.2	6.37
34.2	7.23
68.6	8.51
94.7	9.42
96.7	10.44
9.6	11.76

Figure 25a

Flotation recovery (%)	pH
no additions	
15.3	2.23
30.5	2.98

82.0	4.33
94.0	5.00
98.2	6.00
93.8	6.85
93.8	8.10
94.2	8.94
92.6	10.00
98.8	10.65
15.2	11.65

with 0.6 $\underline{M}$ NaCl

3.8	1.78
9.4	3.80
38.7	5.82
99.6	8.05
98.8	9.93
35.1	11.63

with 0.1 $\underline{M}$ $CaCl_2$

8.3	2.14
25.1	4.04
97.6	6.02
98.2	7.94
93.4	9.88
88.5	11.42

with 0.1 $\underline{M}$ Na_2SO_4

2.6	2.15
7.6	4.15
23.1	6.13
98.0	7.95
99.0	10.05
27.6	11.73

Figure 25b

Flotation recovery (%)	pH
no additions	
15.6	2.23

27.9	4.05
72.6	5.87
96.7	6.95
93.4	8.00
91.5	8.74
95.7	9.85
3.3	11.75

with 0.6 M NaCl

6.1	2.12
11.9	3.97
50.0	6.05
99.7	8.00
99.8	9.95
1.7	11.73

with 0.1 M $CaCl_2$

14.7	2.20
18.9	4.04
80.2	5.98
98.2	8.05
34.5	9.85
39.1	11.43

with 0.1 M Na_2SO_4

3.5	2.33
5.9	4.15
11.8	6.02
96.7	7.93
96.0	10.05
1.3	11.65

Figure 26a

Flotation recovery (%)	pH
Armeen 12D	
1.4	3.98
10.4	6.10

49.8	8.31
98.1	10.61
20.0	11.75
Duomeen 8D	
0.0	2.92
2.3	5.34
11.8	7.24
91.2	9.51
59.2	11.02
Duomeen 12D	
5.5	4.32
20.2	5.45
29.1	5.45
54.5	5.93
72.3	6.48
82.0	7.11
88.5	7.19
91.1	7.50
92.0	8.00
98.5	8.70
99.2	9.68
95.2	10.40
89.0	11.53
Duomeen 16	
9.9	2.12
82.9	3.93
95.7	6.02
98.3	7.40
95.3	9.75
55.9	11.73

Figure 26b

Flotation recovery (%)	pH
Armeen 12D	

0.5	4.60
3.3	6.55
4.4	8.35
27.4	9.41
12.2	10.51
1.0	11.73

WL-

Duomeen 8D

0.0	3.31
0.2	5.53
0.5	7.79
8.8	9.56
1.5	11.28

Duomeen 12D

2.9	2.60
3.8	3.45
4.7	4.47
5.4	5.40
6.9	6.40
14.2	7.65
30.1	8.65
40.3	9.45
16.7	10.52
1.5	11.50

Duomeen 16

3.0	1.95
4.4	3.95
7.8	5.93
22.8	7.00
38.2	8.15
57.6	8.85
6.6	9.92
5.2	10.05
1.5	11.73

Figure 27a

Flotation recovery (%)	pH
Armeen 12D	
4.8	2.82
54.6	5.21
98.7	6.63
98.7	8.55
93.7	10.18
91.2	11.35
Duomeen 8D	
0.6	3.00
12.5	5.18
39.8	6.41
97.5	7.99
99.1	9.00
99.0	10.85
10.5	12.06
Duomeen 12D	
0.7	1.98
5.3	3.10
14.2	3.95
54.6	5.25
91.9	6.02
96.0	6.85
96.1	8.00
97.9	8.93
98.2	10.00
99.0	10.93
100.0	12.25
Duomeen 16	
15.3	2.23
30.5	2.98
82.0	4.33

94.0	5.00
93.2	6.00
93.8	6.85
93.8	8.10
94.2	8.94
92.6	10.00
93.8	10.65
15.2	11.65

Figure 27b

Flotation recovery (%)	pH
Armeen 12D	
6.7	2.51
11.3	4.55
22.6	6.35
80.5	8.32
96.5	10.55
26.4	11.85
Duomeen 8D	
0.0	3.24
0.6	5.22
3.0	7.72
37.2	9.49
7.6	11.41
Duomeen 12D	
10.8	2.51
24.2	3.45
25.4	4.45
32.2	5.44
45.2	6.44
89.4	7.45
89.7	8.72
97.0	9.45
98.5	10.57
96.4	11.55

	Duomeen 16
15.6	2.23
27.9	4.05
72.6	5.87
96.7	6.95
93.4	8.00
91.5	8.74
95.7	9.85
3.3	11.75

Figure 28a

Flotation recovery (%)	pH
Armeen 12D	
1.0	3.50
4.1	6.31
3.6	7.53
13.6	8.51
18.6	9.84
8.6	10.37
2.9	11.52
Duomeen 8D	
0.0	3.31
0.0	6.21
0.0	8.54
0.01	9.85
0.0	11.65
Duomeen 12D	
4.4	1.98
4.6	2.95
4.2	3.98
5.1	5.05
8.6	6.00
12.8	7.13
30.7	8.35
57.9	9.17

37.2	10.15
5.4	11.08
1.7	11.95
Duomeen 16	
0.7	2.15
8.3	3.75
59.6	5.92
90.4	8.00
95.8	10.05
44.0	11.65

Figure 28b

Flotation recovery (%)	pH
Armeen 12D	
0.0	2.53
0.5	4.60
0.7	6.42
0.9	8.45
1.5	10.41
0.4	11.72
Duomeen 8D	
0.0	3.40
0.0	5.34
0.0	7.59
0.0	9.36
0.0	11.27
Duomeen 12D	
1.3	2.80
1.7	3.85
1.5	5.36
2.6	6.36
2.4	7.73
3.5	8.75
2.5	9.33
0.9	10.32

Duomeen 16

3.4	2.00
3.3	4.02
4.3	6.45
9.1	8.00
8.5	9.35
3.3	11.00

Figure 29a

Flotation recovery (%)	pH

Armeen 12D

4.4	3.10
9.6	5.21
26.4	6.51
97.0	7.75
97.8	9.61
77.5	11.41

Duomeen 8D

0.8	1.97
0.9	3.42
2.1	5.33
30.4	7.72
72.3	9.42
3.3	11.33

Duomeen 12D

4.5	2.23
5.3	3.12
13.1	4.17
25.6	5.15
59.7	6.28
97.6	7.34
96.0	8.16
91.3	9.33
99.9	10.25
100.0	11.00
96.5	11.95

Duomeen 16

3.8	1.78
9.4	3.80
88.7	5.82
99.6	8.05
95.8	9.93
85.1	11.63

Figure 29b

Flotation recovery (%)	pH
Armeen 12D	
9.7	2.52
19.5	4.57
25.6	6.40
63.0	8.45
75.6	10.35
6.6	11.57
Duomeen 8D	
0.0	3.31
0.7	5.22
0.7	6.98
1.5	9.30
0.8	11.40
Duomeen 12D	
8.0	2.00
27.8	4.05
35.3	6.05
80.8	7.90
99.0	10.00
18.8	11.85
Duomeen 16	
6.1	2.12
11.9	3.97
50.0	6.05
99.7	8.00

99.8	9.95
1.7	11.73

Figure 30a

Flotation recovery (%)	pH
Armeen 12A	
1.6	3.62
1.9	6.55
10.7	8.64
6.1	10.42
6.9	11.53
Duomeen 8D	
0.0	3.10
0.0	5.50
0.0	7.81
0.0	9.28
0.0	11.21
Duomeen 12D	
2.1	2.13
2.1	3.05
3.2	4.20
7.8	5.13
7.9	6.05
17.2	7.35
33.8	8.30
27.3	9.00
8.6	10.13
8.1	11.40
Duomeen 16	
1.8	2.10
1.6	3.95
2.6	5.95
67.4	8.00
93.4	10.12
4.1	11.88

Figure 30b

Flotation recovery (%)	pH
Armeen 12A	
0.0	2.4
0.2	4.45
0.5	6.51
0.7	8.32
0.7	10.56
0.1	11.65
Duomeen 8D	
0.0	3.70
0.0	5.90
0.0	7.83
0.0	9.21
0.0	11.50
Duomeen 12D	
2.7	4.10
4.3	4.97
2.7	6.05
2.5	7.75
4.0	8.55
1.3	9.92
Duomeen 16	
3.4	2.25
4.2	4.67
5.1	7.75
2.7	9.85
1.9	11.55

Figure 31a

Flotation recovery (%)	pH
Armeen 12D	
5.0	3.81

33.8	6.01
98.7	8.03
97.5	9.81
95.3	11.43

Duomeen 8D

0.0	2.18
1.1	5.03
11.7	7.72
16.4	9.11
5.1	10.39
11.3	11.71

Duomeen 12D

5.0	2.11
11.4	3.17
37.2	4.12
61.5	5.10
81.3	6.15
96.9	7.25
94.1	8.35
92.8	9.24
96.7	10.05
98.7	10.95
98.7	11.95

Duomeen 16

8.3	2.14
25.1	4.04
97.6	6.02
98.2	7.94
93.4	9.88
88.5	11.42

Figure 11b

Flotation recovery (%)	pH

Armeen 12D

6.8	2.55
12.6	4.34
24.4	6.42
20.2	8.80
30.7	10.37
27.8	11.65
Duomeen 8D	
0.0	3.70
0.7	5.51
1.0	7.43
2.3	9.53
0.8	11.52
Duomeen 12D	
13.4	2.72
25.9	3.90
27.9	4.90
34.5	6.08
46.1	7.38
38.7	8.92
61.7	10.50
83.6	11.45
Duomeen 16	
14.7	2.20
18.9	4.04
80.2	5.98
98.2	8.05
34.5	9.85
39.1	11.43

Figure 32a

Flotation recovery (%)	pH
Armeen 12D	
1.8	4.11
3.7	6.15
18.1	8.54

71.3	10.29
6.7	11.75

Duomeen 8D

0.0	3.52
0.5	5.43
0.9	7.12
4.6	9.25
0.0	11.22

Duomeen 12D

2.3	2.55
3.4	3.53
4.8	4.45
5.9	5.45
8.2	6.30
18.9	7.55
43.7	8.65
55.8	9.35
37.3	10.55
10.3	11.50

Duomeen 16

2.3	2.10
3.2	4.15
3.8	6.00
4.4	7.75
4.0	9.85
1.5	11.65

Figure 32b

Flotation recovery (%)	pH

Armeen 12D

0.3	2.71
0.5	5.12
0.7	7.63
0.9	8.71

1.4	10.45
0.6	11.69
Duomeen 8D	
0.0	3.16
0.1	4.54
0.0	6.85
1.4	9.29
0.0	10.93
Duomeen 12D	
2.3	2.25
2.7	3.25
3.7	4.25
2.7	5.25
3.3	7.15
1.4	9.35
4.4	10.95
Duomeen 16	
2.3	2.10
3.2	4.15
3.8	6.00
4.4	7.75
4.0	9.85
1.5	11.65

Figure 33a

Flotation recovery (%)	pH
Armeen 12D	
4.3	2.99
13.2	5.41
44.2	7.19
98.3	8.11
97.5	10.01
98.04	11.61

Duomeen 8D

0.3	2.21
0.4	3.83
1.8	5.37
4.5	6.94
95.4	9.52
37.5	10.91

Duomeen 12D

4.4	2.15
32.7	3.45
68.2	4.50
79.9	5.45
88.5	6.35
95.7	7.40
91.0	8.35
93.2	9.35
97.5	10.35
99.8	11.50

Duomeen 16

2.6	2.15
7.6	4.15
23.1	6.13
98.0	7.95
99.0	10.05
27.6	11.73

Figure 33b

Flotation recovery (%)	pH
Armeen 12D	
14.1	2.62
21.5	4.53
28.7	6.53
72.7	8.62
99.3	10.53
9.3	11.73

Duomeen 8D

0.4	4.50
0.3	5.80
0.7	7.67
1.5	9.58
0.2	10.91

Duomeen 12D

15.8	2.05
41.1	4.05
59.1	6.00
89.5	8.25
97.5	9.95
35.4	11.95

Duomeen 16

3.5	2.33
5.9	4.15
11.8	6.02
96.7	7.93
96.0	10.05
1.3	11.65